PALEOCEANOGRAPHY, VOL. 9, NO. 6, PAGES 835-855, DECEMBER 1994

Magnetostratigraphic, biostratigraphic, and stable isotope stratigraphy of an Upper Miocene drill core from the Salé Briqueterie (northwestern Morocco): A high-resolution chronology for the Messinian stage

David A. Hodell,[1] Richard H. Benson,[2] Dennis V. Kent,[3] Anne Boersma,[4] and Kruna Rakic-El Bied[5]

Abstract. We report a high-resolution stable isotope, carbonate, magnetostratigraphic, and biostratigraphic record from a 175-m drill core from the Salé Briqueterie, which is part of the Bou Regreg section in northwestern Morocco. The Salé drill core spans the interval from paleomagnetic Chron C4n partim to C3r (earliest Gilbert), which represents the time leading up to and including the isolation and desiccation of the Mediterranean (i.e., the Messinian salinity crisis). During Chrons C3An and C3Ar (6.935 to 5.894 Ma) the isotope and carbonate signals display quasi-periodic variations with estimated periods of 40 and 100 kyr, respectively. We interpret the 40-kyr $\delta^{18}O$ variations as reflecting changes in global ice volume caused by obliquity-induced changes (41 kyr) in solar insolation in polar regions. The 100-kyr carbonate variations probably represent long-term modulation of the amplitude of the precessional cycle (~21 kyr), which is not resolved by our sampling frequency. The cyclic nature of the oxygen isotope signal permits us to extend the isotope nomenclature of Shackleton et al. (1994a) from stage TG24 in Chron C3r (earliest Gilbert) to stage C3Ar.$\delta^{18}O$.18 at the base of Chron C3Ar (6.935 Ma). A major change in paleoceanographic conditions is recorded across the Tortonian/Messinian boundary, which we correlate to Chron C3Bn at 7.04 Ma. Benthic foraminiferal $\delta^{18}O$ values increased by an average of 0.4‰ in two steps at 7.17 Ma and 6.8 Ma and $\delta^{13}C$ values decreased by 0.7-0.8‰ between 7.1 and 6.8 Ma, representing the late Miocene carbon shift. The first step in $\delta^{18}O$ values coincides with an inferred reversal in deep water circulation through the Rifian Corridor, and the second correlates with the base of the Tripoli Formation and onset of "crisis conditions" in the Mediterranean. We suggest that the increase in $\delta^{18}O$ values represents, at least in part, an increase in global ice volume that lowered sea level and contributed to the establishment of a negative water budget in the Mediterranean. Average $\delta^{18}O$ values remained high throughout most of Chrons C3Ar and C3An, reaching maximum $\delta^{18}O$ values during isotope stages TG20 and 22 in Chron C3r (earliest Gilbert). The glacio-eustatic falls associated with these events may have resulted in the complete isolation of the Mediterranean from the world ocean (Shackleton et al., 1994a). Following stage TG12 in the Salé record, there exists a trend toward progressively lower $\delta^{18}O$ values that may represent a series of marine transgressions that eventually reflooded the Mediterranean and ended the Salinity Crisis.

Introduction

Ever since the discovery over 20 years ago that the Mediterranean Sea had been isolated from the world ocean during the late Miocene, the "Messinian salinity crisis" has captured the attention and imagination of the scientific and lay communities [*Hsü*, 1972; *Hsü et al.*, 1973]. The isolation and desiccation of the Mediterranean was an event of profound consequence that is without parallel in the modern world [*Benson*, 1991; *Benson and Rakic-El Bied*, 1991a]. The salinity of the oceans is held constant over long periods of geologic time by the episodic evaporation of seawater and deposition of salts in isolated basins. Evaporite deposition represents the primary sink for some of the major ions in seawater including sodium, chloride, and sulfate. The isolation and desiccation of a marginal basin of sufficient volume to affect ocean salinity is a chance event that does not occur predictably in time. The Messinian salinity crisis is the most recent of such events that adjusted the ocean's salinity by removing an estimated 6% of dissolved salts from seawater [*Ryan et al.*, 1974]. After 20 years of study the global implications and ramifications of this reduction in oceanic salinity by 2‰ are still not completely understood.

One of the problems that has hampered study of the Messinian salinity crisis, both within and outside of the Mediterranean, has been the difficulties associated with stratigraphy and chronology. The fact that the Mediterranean was isolated from the world ocean during the latest Miocene has made stratigraphic correlation

[1]Department of Geology, University of Florida, Gainesville.
[2]Smithsonian Institution, U.S. National Museum, Washington, D.C.
[3]Lamont-Doherty Earth Observatory, Palisades, New York.
[4]Microclimates, Research Consultants, Stony Point, New York.
[5]Smithsonian Institution, Rabat, Morocco.

Paper number 94PA01838.
0883-8305/94/94PA-01838$10.00

difficult. During the salinity crisis, environmental conditions within the Mediterranean excluded most marine microfossil groups that are traditionally used for biostratigraphic correlation. In addition, the lithologies of the evaporitic deposits themselves are generally not amenable to radiometric dating or paleomagnetic analysis. Strontium isotope stratigraphy has been of limited value in correlating and dating the lower evaporites, but the resolution of this technique is poor (±0.5 m.y.) and the upper evaporites were found to have nonmarine $^{87}Sr/^{86}Sr$ signatures [*Müller and Mueller*, 1991].

Because sequences deposited within the Mediterranean during the salinity crisis are inherently discontinuous, we must look outside the Mediterranean to find continuous, marine sequences of the Messinian stage. Upper Miocene sequences in the Bou Regreg Valley of northwestern Morocco have been important historically for reconstructing the history of the Messinian salinity crisis because they were deposited in one of two gateways that controlled the exchange of marine waters between the Atlantic and Mediterranean [*Feinberg and Lorenz*, 1970; *Cita and Ryan*, 1978a; *Hodell et al.*, 1989; *Benson et al.*, 1991]. Sedimentation was not interrupted during the salinity crisis because these sequences were located on the Atlantic side of the Mediterranean. As a result, these marine deposits chronicle the history of oceanic conditions during the salinity crisis and serve as important stratigraphic links between Mediterranean and deep sea sequences.

Here we present a high-resolution stable isotope and carbonate stratigraphy from a continuous 175-m drill core from the Salé Briqueterie, northwestern Morocco. The clear paleomagnetic, oxygen isotope and carbonate signals from this core permit us to extend the isotope nomenclature of *Shackleton et al.* [1994a] from stage TG24 (the oldest stage identified in site 846) during Chron C3r to stage C3Ar.$\delta^{18}O$.18 at the base Chron C3Ar (6.935 Ma). This record provides a high-resolution stratigraphy for the Messinian stage, which can be used to improve our understanding of the relationships among stable isotope changes, global ice volume, sea level, and the Messinian salinity crisis.

Materials and Methods

Drill Cores

The cores used in this study were obtained from a large brick quarry (the Salé Briqueterie) found on the road to the airport just east of Rabat, Morocco (Figure 1). The drilling at Salé was accomplished for us in two phases in April 1987 and September 1988 under contract to SOLMAROC, a local drilling company. The section was cored by continuous "mazier" drilling (cookie cutter bit) with 1-m core barrel that was 74 mm in diameter. During the first drilling, 72 cores were recovered to a maximum depth of ~75 m below the quarry floor. These cores are designated the S series. During the second phase of drilling the first 60 m were drilled without recovery and 104 cores were recovered below this level reaching a maximum depth of approximately 170 m. These cores are designated the B-series. The lowest part of the B series was drilled by destructive rotary drilling and only spot cores were obtained. The overlap between the S and B series drilling is about 7 m (between 66 and 73 m below the base of the quarry floor). The depth offset between the two holes is ~5 m and this amount was added to all of the core depths measured in the field for the B series samples.

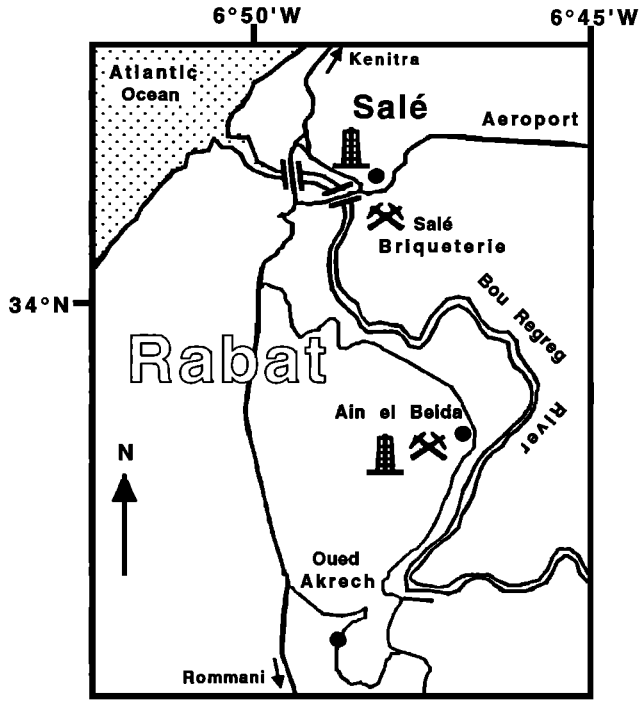

Figure 1. Location of the Bou Regreg section near Rabat on the Atlantic Coast of Morocco including the Salé Briqueterie Quarry where the cores used in this study were taken. Other sections previously studied include the Ain el Beida Quarry and Oued Akrech Road Section.

The sampling of the cores began by dividing each 1-m-long core into two halves of approximately equal length. The upper ~0.5 m was designated as the archive half of the core and was retained by the Moroccan Geological Survey. Only the lower 0.5 m of each core was sampled to avoid possible downhole contamination. Although the lower half of each core was sampled at a frequency greater than every 50 cm, the unsampled archive half of the core limits the even sample spacing to 50 cm. Coring operations at Salé were not originally designed with high-resolution paleoceanographic studies in mind, and so this study is limited by the rather coarse coring and sampling methods employed. Normally, in deep-sea cores this wide sampling interval would severely hamper the chances of obtaining a high-resolution record but, by comparison, the sedimentation rates in the Salé core are high. During Chrons C3An and C3Ar where the age control is excellent, sedimentation rates averaged about 5 cm/kyr which translates into an average sample spacing of about 10,000 years.

The highest frequency that can be resolved by the data set is equivalent to a period of about 20,000 years (i.e., the Nyquist frequency) assuming that each record was sampled at a constant time step of 10,000 years. Ideally, the time series should be sampled at 4-kyr resolution to confidently resolve precessional periods of 19 and 23 kyr. Aliasing of a time series by sampling at an interval that is too great to adequately resolve the true nature of a periodic signal may shift variance into lower frequencies [Pisias and Mix, 1988]. As a result, the sampling interval of the Salé core limits the interpretation of the results at the high end of the

Milankovitch frequency band (i.e., precessional 19 and 23 kyr), but is adequate to resolve lower frequencies (i.e., obliquity and eccentricity).

Paleomagnetics

Full-round samples oriented with respect to the vertical (but an arbitrary azimuth) were taken at nominal 50-cm intervals from the S series and B series cores and prepared for paleomagnetic analysis by subsampling into ~15 cm^3 specimens. Magnetic remanence measurements (made with a ScT or 2G cryogenic magnetometer) and demagnetization experiments were performed in a magnetically shielded environment with fields less than 5 nT over the sample space during the procedures. The intensities of natural remanent magnetism (NRM) ranged widely, averaging about 3 mA/m but with half the samples, mostly in the S series cores, having intensities less than 1 mA/m. A set of subsamples was initially subjected to progressive alternating field demagnetization to 100 mT but thermal demagnetization was found to give more complete separation of magnetization components contributing to the NRM and was used as the basis of polarity interpretation.

The NRM demagnetization behavior can be generally categorized as stable for the B series but typically unstable for much of the stratigraphic interval covered by the S series cores. Representative samples of stable behavior in the B series cores are illustrated in Figures 2a-2d. Spurious magnetizations or present-day field overprints, if present, were typically removed by 300°C to reveal a univectorial, characteristic magnetization to treatment levels of 600°C, with either negative (Figures 2a and 2c) or positive (Figures 2b and 2d) inclination. The unblocking temperatures, which were concentrated between 500° and 600°C, are consistent with magnetite as the principal carrier of the NRM. However, there is typically a small fraction of remanence remaining after the 600°C treatment step which may reflect a minor contribution from hematite. The presence of high coercivity hematite, which has been confirmed in isothermal remanent magnetization (IRM) acquisition and thermal demagnetization experiments, may explain why alternating field demagnetization was less effective than thermal treatment in resolving the characteristic magnetization. Similar magnetic properties have been described for upper Miocene sediments from Morocco by *Moreau et al.* [1985].

Most (but not all) of the S series samples showed poor demagnetization behavior (e.g., Figures 2e-2g). Samples with unstable behavior are usually characterized by very low NRM intensities (~0.1 m/Am) which are reduced by an order of magnitude and/or have inconsistent directions by 400° or 450°C. Magnetic susceptibility typically increases substantially after the 400°C treatment, suggesting magnetochemical alteration during demagnetization. Large susceptibility increases at about 400°C also occur in samples with stable demagnetization behavior but are usually not catastrophic in terms of the recovery of stable,

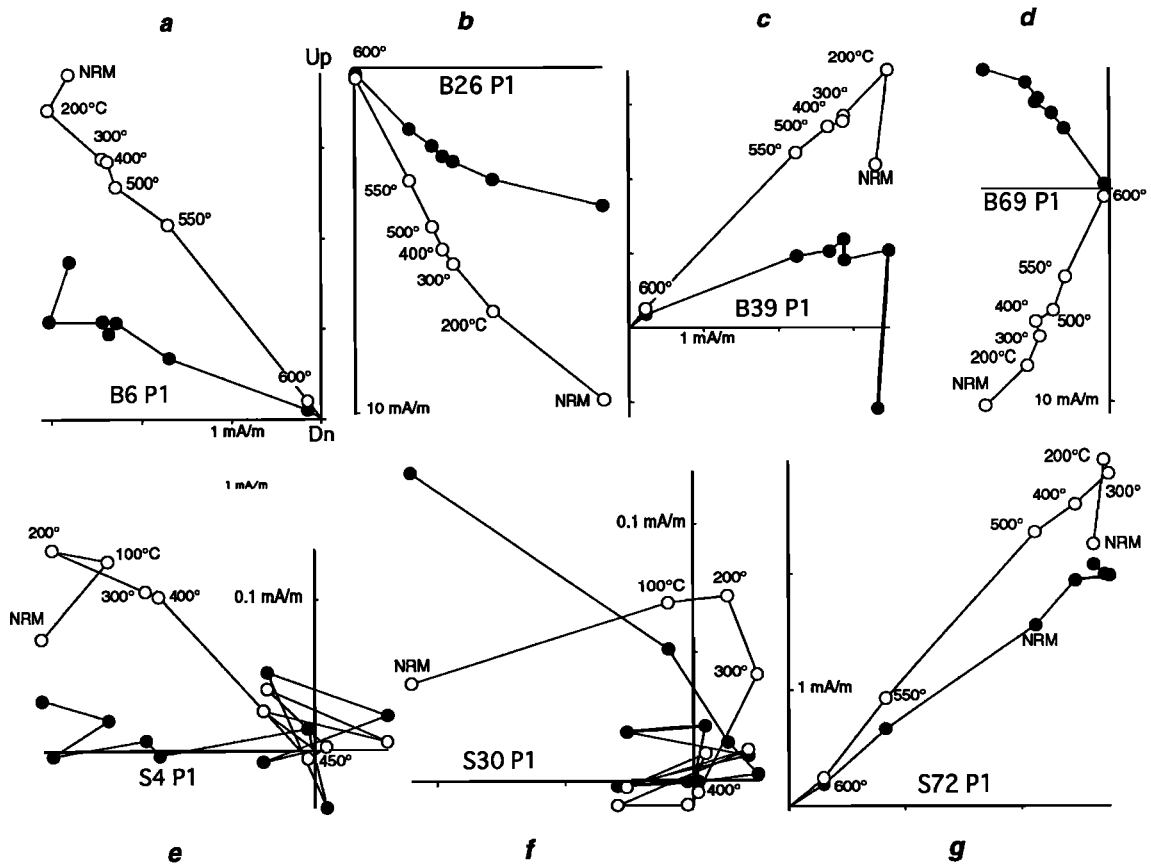

Figure 2. Representative vector endpoint demagnetograms showing change in NRM with progressive thermal demagnetization of samples from the B series (a to d) and S series (e to g) cores. Open (closed) symbols are projections of magnetization vector on vertical (arbitrary horizontal) axis after each demagnetization step.

characteristic directions. Two intervals from the S series (from cores 37 to 53 and from about cores 63 to 72), however, have generally higher NRM intensities and show more stable demagnetization behavior (Figure 2g), similar to what has been described as typical for most of the B series samples. The magnetic instability so common in the S series, but that is much less so in the B series (except below 154 m), is therefore not attributed to some peculiarity of coring or sample processing, but rather is believed to be a stratigraphic-dependent property of these sediments.

Principal component analysis [*Kirschvink*, 1980] was used to identify and calculate characteristic directions based on consistency of demagnetization results in the 500° to 600°C treatment interval. This procedure effectively eliminated from further consideration samples with erratic directional behavior above 400°C; these are indicated by crosses along the 0° inclination axis in Figure 3. The characteristic inclination directions delineate normal and reversed polarity intervals that are taken to represent the polarity of the geomagnetic field near to the time of deposition (Figure 3). The mean inclinations (48°±11° for normal, -40°±11° for reversed) are somewhat shallower than the dipole field inclination (±53.5°) for the site latitude but are consistent with respect to the Miocene paleomagnetic field for Africa (e.g., mean Miocene pole of *Tauxe et al.* [1983] would predict an inclination of ±44°).

Stable Isotopes

Isotope measurements were made on the benthic foraminifera, *Planulina ariminensis*, which has a modern depth distribution between 300 and ~1000 m [*Lutze*, 1980]. *Planulina ariminensis* is considered to be the shallow-water equivalent of *Planulina wuellerstorfi*, which is the preferred species for deep sea isotope studies. Isotope comparisons of *P. ariminensis* and *P. wuellerstorfi* have found a small, consistent offset of 0.3‰ for $\delta^{18}O$ and 0.2‰ for $\delta^{13}C$ between the two species [*Zahn et al.*, 1987].

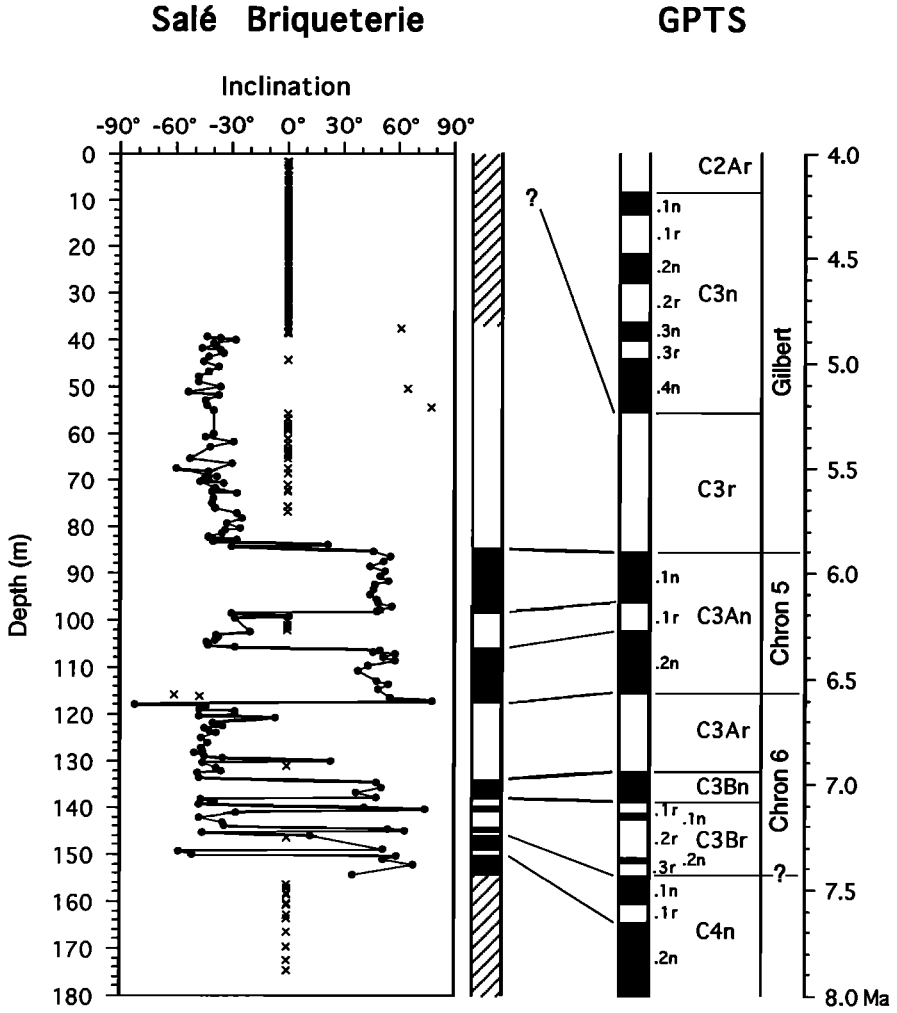

Figure 3. Paleomagnetic results from the Salé core showing inclination data, interpretation of normal and reversed polarity intervals, and correlation to the geomagnetic polarity timescale of *Cande and Kent* [1992, submitted manuscript, 1994]. Crosses represent data that were not considered in polarity interpretation because of either weak, unstable magnetizations (arbitrarily assigned 0° inclination) or suspected problems with overprints or core handling. Magnetostratigraphic chron nomenclature for polarity intervals older than the Gilbert (e.g., Chrons 5 and 6) is shown for reference only and is superseded by the chron nomenclature derived from magnetic anomalies.

About 5 to 10 specimens of *P. ariminensis* were selected for isotope analysis such that samples weights were approximately 400-500 μg of carbonate per analysis. In many samples, *P. ariminensis* was abundant enough to make duplicate isotope measurements from the same sample and the results were averaged to reduce the noise level of the data. This is desirable because the amplitude of the $\delta^{18}O$ signal is low (0.5-0.6 ‰) during the late Miocene. Foraminiferal tests were reacted in a common acid bath of ortho-phosphoric acid at 90°C using a VG Isogas autocarbonate preparation system. Isotope ratios of purified CO_2 gas were measured on-line by a VG Prism Series II mass spectrometer. All isotope results are reported in standard delta notation relative to PDB (Appendix Tables A1 and A2, which are available from the National Geophysical Data Center, Boulder, Colorado, at paleo@mail.ngdc.noaa.gov). Analytical precision, based upon routine analysis of an internal carbonate standard (Carrara Marble), was ±0.07 for $\delta^{18}O$ and ±0.03 for $\delta^{13}C$. Sample reproducibility of the results (as measured by the mean and standard deviation of the absolute value of the difference between 292 replicate analyses) was estimated to be 0.09 ±0.08‰ for $\delta^{18}O$ and 0.17 ±0.14 for $\delta^{13}C$.

Carbonate

For measurement of percent $CaCO_3$, bulk samples were ground to a homogeneous powder and acidified by reaction with 2N HCl in a closed system using nitrogen as a carrier gas. Carbon dioxide generated from the reaction was introduced into a cell and measured by coulometric titration using a UIC Model 5011 carbon analyzer [*Engleman et al.*, 1985]. Precision is estimated to be ±1% (±1 standard deviation) based on repeated analysis of reagent-grade $CaCO_3$.

Results

Magnetic Polarity Stratigraphy

The polarity reversal pattern from the B series drilling at Salé can be correlated to the geomagnetic polarity timescale (GPTS) of *Cande and Kent* [1992] from Chron C3r (the early Gilbert) to the top of Chron C4n partim (Figure 3; Table 1). The Chron C3An/C3r boundary (Chron 5/Gilbert) is recognized at 84.83 m (corrected depth) and all subchrons of C3An are clearly defined. There are two possible solutions for placement of the base of Chron C3An.2n owing to the likelihood of inversion of either core 50 or 51. If core 50 was inverted, then the polarity reversal occurs at 117.4 m. If core 51 was inverted, then the base of C3An.2n is located at 115 m. On the basis of cyclostratigraphy (see discussion below), we favor the former position at 117.4 m. Below this level, the correlation of Chron C3Ar and C3Bn at Salé to the GPTS is reasonably clear. Chrons C3Br and C4n partim can also be recognized in the condensed lower part of the section before unstable magnetizations prevent further polarity determinations below about 154 m (Figure 3).

In comparison to the B series samples, the overall quality of the magnetic data in the S series samples is poor. Thermal demagnetization revealed that S series samples were either reversed polarity or showed unstable behavior above 400°C treatment (although magnetizations with negative inclination were sometimes apparent at lower unblocking temperatures as in Figures 2e and 2f). The reversed polarity interval below 40 m is correlated to Chron C3r (earliest Gilbert; Figure 3). Above 40 m, all samples showed unstable behavior upon thermal demagnetization, and no polarity interpretation is possible. As a result, we were unable to determine if the oldest normal polarity interval of the Gilbert (i.e., Thvera Subchron or C3n.4n) is present in the S series samples.

Biostratigraphy

A consistent planktonic calcareous biostratigraphy has been developed in outcrop and cored sections in the Bou Regreg Valley at Oued Akrech, Ain el Beida, the Salé Briqueterie (Figure 4), and at outcrops to the east at Ain Allal ben Mehdi and Oued Arjat [*Benson et al.*, 1991; *Benson and Rakic-El Bied*, 1991a]. This biostratigraphy has been calibrated directly to the geomagnetic

Table 1. Stratigraphic Position and Ages of Normal Polarity Intervals Used to Construct Age Model for the B Series Samples in the Salé Briqueterie Core

Chron	Position	Sample Range	Depth Range	Mean depth	Age*	Age†
C3An.1n	top	P1-19 to P1-20	84.35-85.3	84.83	5.875	5.894
	base	P2-32 to P1-33	98.19-98.7	98.45	6.122	6.137
C3An.2n	top	P1-40 to P2-40	105.8-106.34	106.07	6.256	6.269
	base	P2-51 to P1-52	117.09-117.7	117.4	6.555	6.567
C3Bn	top	P1-67 to P2-68	133.5-134.6	134.05	6.919	6.935
	base	P1-71 to P2-17	137.7-138.25	137.98	7.072	7.091
C3Br.1n	top	P2-72 to P1-73	139.29-139.85	139.57		7.135
	base	P2-73 to P2-74	140.34-140.85	140.60		7.170
C3Br.2n	top	P1-77 to P2-77	143.9-144.4	144.17		7.341
	base	P1-78 to P2-78	145.0-145.49	145.25		7.375
C4n.1n	top	P2-78 to P1-79	145.49-145.95	145.72		7.432
	base	P2-82 to P2-82	148.85-149.39	149.12		7.562
C4n.2n	top	P2-83 to P2-83	149.85-150.39	150.12		7.650

*Shackleton et al. [1994b].
†Cande and Kent [1992, submitted manuscript, 1994].

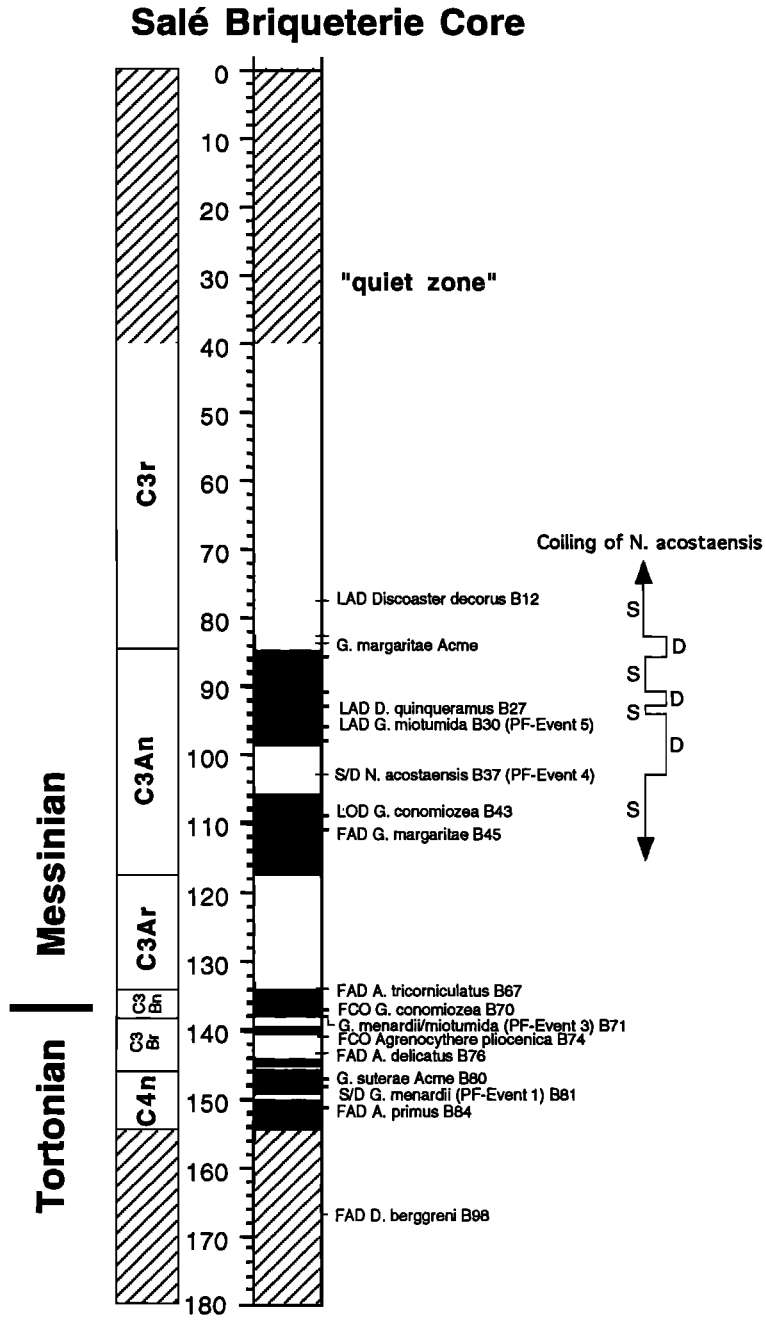

Figure 4. Position of important calcareous biostratigraphic events in the Salé core relative to depth (in meters) and to the interpretation of the magnetic results presented in Figure 3. Numbers following species names represent the identification number from the B series samples in which the datum was found. PF-Event designations are after *Sierro et al.* [1993]. FAD, first appearance datum; S/D, coiling direction change from sinistral to dextral; D/S, coiling direction change from dextral to sinistral; FCO, first common occurrence; LAD, last appearance datum; LOD, last occurrence datum.

polarity time scale and provides a high-resolution biomagnetostratigraphy, especially for the time interval leading up to the Messinian salinity crisis.

Planktonic foraminifera. During the late Miocene a major turnover occurred in globorotaliid foraminiferal assemblages in the northeast Atlantic and Mediterranean [*Sierro*, 1985; *Benson and Rakic-El Bied*, 1991a, b; *Sierro et al.*, 1993]. This event was marked by a replacement in dominance of the subtropical menardines with the temperate, conic globoconellids. Planktonic foraminiferal biostratigraphy during the late Miocene is based on morphological and species assemblage changes associated with this replacement along with first and last appearances or occurrences of species. The following events are considered the most important:

1. A change in coiling direction from sinistral to dextral *Globorotalia menardii* (PF-Event 1 of *Sierro et al.* [1993]). This event marks a southward retreat of this form in the North Atlantic and is recognized in the Salé core at 148.15 m in Subchron C4n.1n (Figure 4).

2. The presence of the acme of *Globorotalia suterae* which occurs in Subchron C4n.1n in the Salé core (Figure 4). This biostratigraphic event permits correlation between the Italian Tortonian stratotype sequence and the Atlantic.

3. A pronounced change in late Miocene globorotaliid assemblages involves the replacement of the *Globorotalia menardii* group by the *Globorotalia miotumida* group (PF-Event 3 of [*Sierro*, 1985]). This event represents a change between an epipelagic fauna with a tropical to subtropical affinity to that of a mesopelagic fauna of temperate affinity, marking a southward migration of northern temperate faunas in the North Atlantic [*Sierro*, 1985]. At Salé this event is recognized at 138 m at the base of Chron C3Bn, just below the Tortonian/Messinian boundary.

4. The First Common Occurrence (FCO) of *Globorotalia conomiozea*, used to identify the Tortonian/Messinian boundary, occurs within Chron C3Bn at 136.7 m at Salé (7.04 Ma). We use the typical conic form of *G. conomiozea* for this identification [*Scott*, 1980]. This biohorizon was recognized also in Chron C3Bn at site 654 in the Tyrrhenian Sea [*Channell et al.*, 1990a]. In Crete, however, *Krijgsman et al.* [1994] correlated the Tortonian/Messinian boundary to the reversed interval of Subchron C3Br.1r on the basis of the first appearance of an early stage of development of *G. conomiozea*. Because of difficulties with the geomagnetic measurements at Falconara in Sicily [*Langereis and Dekkers*, 1992], the correlation of the FCO of *G. conomiozea* to the GPTS in the neostratotype remains uncertain.

5. The evolution of the *Globorotalia margaritae* lineage allows us to identify several evolutionary stages between *G. margaritae primitiva* and *G. margaritae sensu stricto* before the salinity crisis [*Benson and Rakic-El Bied*, 1991b]. In the Salé core the FAD of *G. margaritae sensu stricto* occurs in Chron C3An.2n and an acme of *G. margaritae* occus near the C3An/C3r boundary (Figure 4).

6. The first change in coiling direction of *Neogloboquadrina acostaensis* (from sinistral to dextral) and the FAD of *Discoaster quinqueramus* are the last two bioevents recognized in the Mediterranean before the onset of evaporite deposition [*Bizon and Bizon*, 1972; *Stainforth et al.*, 1975; *Zachariasse*, 1975; *Colalongo et al.*, 1979; *Sierro*, 1985; *Cita and McKenzie*, 1986]. In the Ain el Beida section one finds at least five alternations in coiling direction of *N. acostaensis* starting late in Subchron C3An.1r. At Salé the first coiling change (S/D) is found at 102.85 m, also in Chron C3An.1r (Figure 4). Five other shifts occur at approximately 94 m (D/S), 92.9 m (S/D), 90.8 m (D/S), 85.6 m (S/D), and 82.6 m (D/S). Above the last coiling shift in Chron C3r, the coiling of *N. acostaensis* remains dominantly sinistral for the remainder of the core record. *Stainforth et al.* [1975] reported the first change in coiling direction near the top of the diatomite section of the Tripoli Formation at Falconara (before the FAD of dwarfed *Globigerina multiloba, Colalongo et al.* [1975]). *Bossio et al.* [1976] reported the coiling shift just a few meters below the evaporites at Ripa dello Zolfo (Piedmont, northern Italy). Other studies have reported the change in C3An from the Pacific [*Saito et al.*, 1975; *Keigwin and Shackleton*, 1980]. In the North Atlantic, coiling changes extend higher into the Gilbert [*Hooper and Weaver*, 1987] and have also been found just below the Thvera Subchron in the Trubi Formation in Sicily (*F. J. Hilgen*, personal communication, 1994).

7. The last appearance (LAD) of *Globorotalia miotumida* (PF-Event 5 of *Sierro et al.* [1993]) occurs at 95.9m near the base of Chron C3An.1n in the Salé core (Figure 4). This bioevent has been found just after the first change in coiling direction of *N. acostaensis* in Morocco, the north Atlantic, and just below the Calcare di Base and lower evaporites in the Mediterranean.

An interval without biostratigraphic events (we call the biostratigraphic "quiet zone") extends throughout much of the long interval of reversed polarity in the earliest Gilbert (Chron C3r). The lack of biomarkers during this period hinders stratigraphic correlation near the top of the Salé core and poses a problem for global correlation of the Miocene/Pliocene boundary [Benson and Hodell, 1994]. The only constraint, albeit indirect, imposed by the biostratigraphy of the S series samples at Salé is that the top of the core is older than the FAD of *G. puncticulata*, which has been found to first occur in Subchron C3n.2n (Nunivak) [*Thunell et al.*, 1991; *Channell et al.*, 1990a].

Calcareous nannoplankton. The following events can be identified in the Salé core from the distribution of calcareous nannoplankton species.

1. The FAD of *Amaurolithus primus* occurs in the upper Tortonian during C4n.2n (Figure 4).

2. The FAD of *A. delicatus* occurs in C3Br.2r and predates the FCO of *G. conomiozea*, as it does in Mediterranean sequences in the Piedmont and Sicilian basins [*Colalongo et al.*, 1979] and at the type Andalusian section at Carmona [*Flores*, 1985].

3. The FAD of *A. tricorniculatus* was found near the Subchron C3Ar/C3Bn boundary at 6.935 Ma in the sequences at Ain el Beida, Salé (Figure 4), and Oued Akrech. We consider the FAD of *A. tricorniculatus* to be an earliest Messinian event, just prior to the onset of the Salinity Crisis. In the Mediterranean, *A. tricorniculatus* first occurs as rare speciments just below the Tripoli Formation in Sicily.

4. The LAD of *Discoaster quinqueramus* was found at Salé in the middle of Subchron C3An.1n, which is the same correlation reported from site 397 off Morocco [*Mazzei et al.*, 1979]. It post dates the first change in coiling direction of *N. acostaensis* (PF-Event 4) and the LAD of *G. miotumida* (PF-Event 5) (Fig. 4). The LAD of *D. quinqueramus* cannot be precisely determined in the Mediterranean because of the presence of the salinity crisis. It ranges to the top of the Tripoli Formation in Sicily and Tuscany [*Bossio* et al., 1985]. Rare specimens have been found in the Arenazzolo Formation at site 132, but these are considered to be reworked.

Oxygen Isotope Measurements

The oxygen isotope signal is marked by long term trends that are superimposed upon quasi-periodic variations (Figure 5) From the base of the section to 150 m, $\delta^{18}O$ values average about 0.8‰. From 150 to 140 m during the late Tortonian there is a brief interval where mean $\delta^{18}O$ values are distinctly lower by about 0.2‰ (averaging about 0.6‰). From 140 to 125 m across the Tortonian/Messinian boundary, $\delta^{18}O$ values increase and average 1.1 to 1.2‰ between 125 and 53 m. Mean $\delta^{18}O$ values are enriched by about 0.4‰ during this interval and distinct glacial-interglacial cycles are superimposed upon the overall high mean values of the $\delta^{18}O$ signal. Glacial $\delta^{18}O$ values commonly reach 1.3 ‰, whereas minimum interglacial values average about 0.8‰.

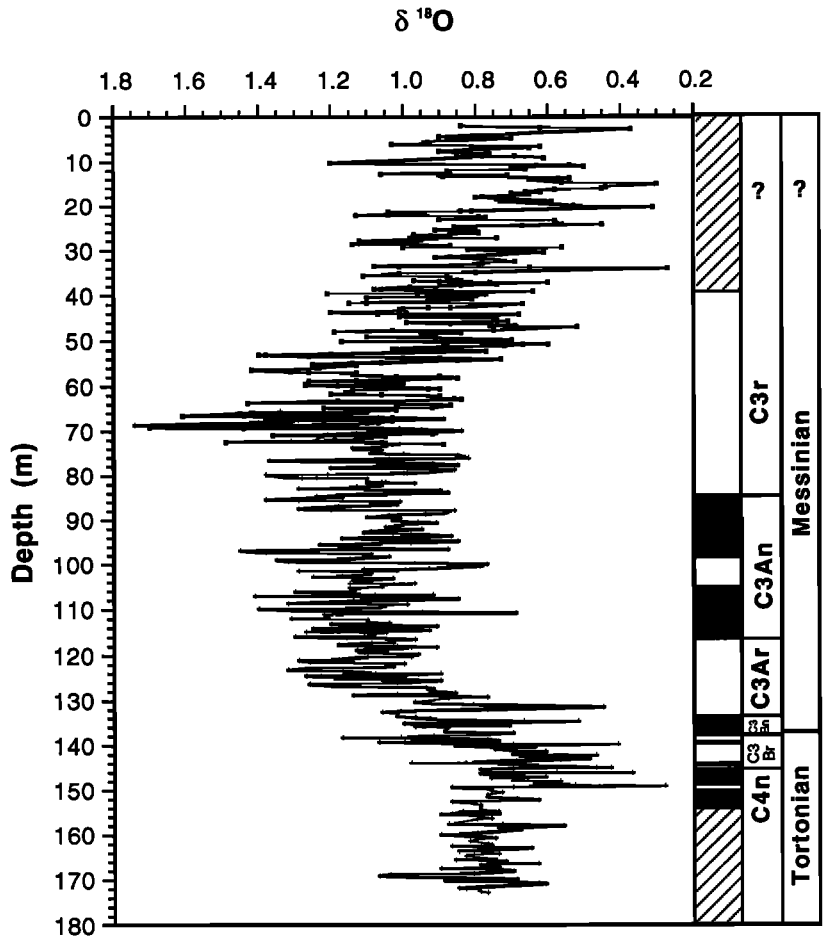

Figure 5. Oxygen isotopic results of the benthic foraminifera, *Planulina ariminensis*, from the B series (crosses) and S series (squares) samples from the Salé core. Note the increase in $\delta^{18}O$ values across the Tortonian/Messinian boundary during Chrons C3Bn and C3Ar. Maximum $\delta^{18}O$ values occur at 68m in Chron C3r. Above 52m, $\delta^{18}O$ values progressively decrease toward the top of the core.

The range of the signal is about 0.5 to 0.6‰ in this interval. The greatest $\delta^{18}O$ values of the entire late Miocene occur between 66 and 70 m in Chron C3r (earliest Gilbert). At ~52 m in Chron C3r, mean $\delta^{18}O$ values decrease by ~0.3‰ and minimum $\delta^{18}O$ values become progressively lower toward the top of the core reaching values as low as 0.3 to 0.4‰.

Carbon Isotope Measurements

From 175 to 140 m, $\delta^{13}C$ values average about 1.3‰ although there are distinct intervals of both higher and lower values in this interval (Figure 6). For example, a short interval of enriched $\delta^{13}C$ values, averaging 1.6‰, is found between 152 and 146 m. From 140 to 130 m across the Tortonian/Messinian boundary, $\delta^{13}C$ values decrease by about 1‰ marking the late Miocene carbon shift. A series of minimum $\delta^{13}C$ values follows the carbon shift between 130 and 120 m. Above 110 m, mean $\delta^{13}C$ values increase slightly and average ~0.8‰ for the remainder of the record.

Percent Carbonate Measurements

The carbonate signal was smoothed with a 3-pt running mean to emphasize long-term variations (Figure 7). Percent carbonate in the Salé core varies from high values of 70 to 75% in the lower part of the core to low values of ~40% at the top of the core (Figure 7). The carbonate signal is marked by cyclic changes superimposed upon longer-term trends. From 175 to 65 m, carbonate content of the sediment is relatively high, averaging about 60% (Figure 7). From 65 m to the top of the section the carbonate signal is marked by a trend toward progressively lower values reaching a minimum of 40% at the top of the core.

Magnetic Susceptibility Measurements

Magnetic susceptibility in the Salé core varies by a factor of 5 and averages about 11 x 10^{-5} SI volumetric units (Figure 8). The magnetic susceptibility variation, however, does not correspond well to that of carbonate percentages, showing only a very weak inverse correlation (r=0.18) with little indication of even an overall trend that might be related to the upward general decrease in carbonate content (Figure 7). The prominent variations in magnetic susceptibility are therefore unlikely to be due to variable dilution by the nonmagnetic carbonate fraction and may instead reflect changes in the concentration or type of magnetic material within the terrigenous fraction, perhaps due to diagenesis.

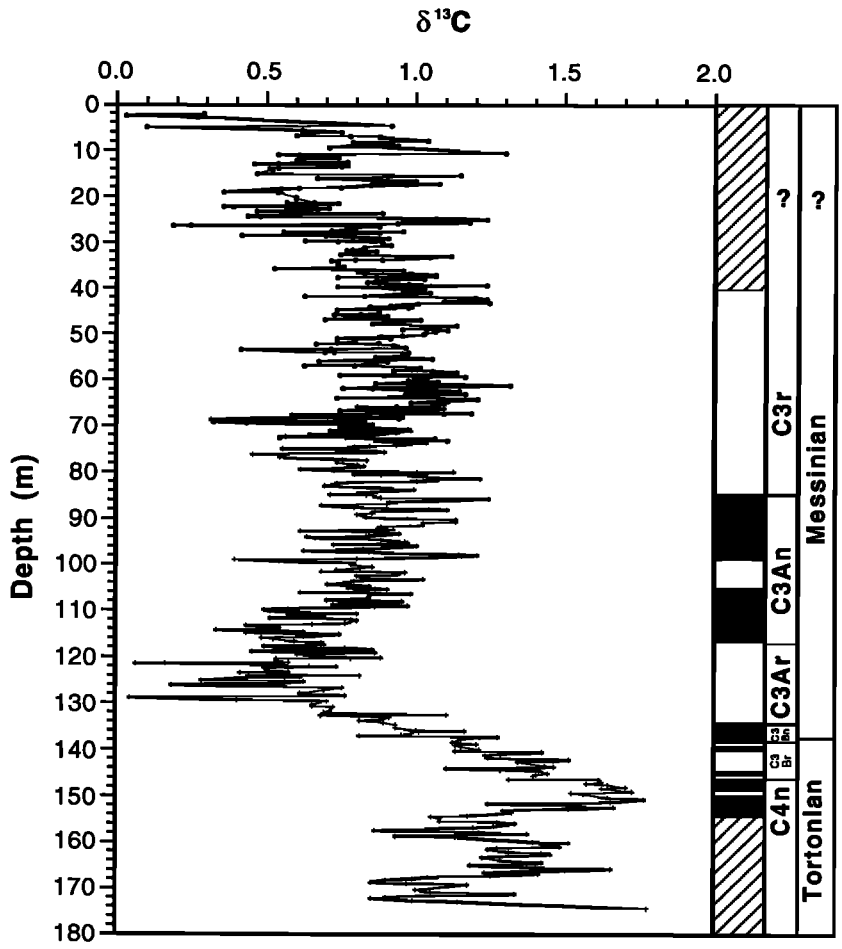

Figure 6. Carbon isotopic results of the benthic foraminifera, *Planulina ariminensis*, from the B series (crosses) and S series (squares) samples from the Salé core. Note the decrease in $\delta^{13}C$ values near the Tortonian/Messinian boundary, which represents the late Miocene carbon shift.

Intervals characterized by low magnetic susceptibility (0-40 m, 55-75 m, 150-175 m) are generally associated with weak, less stable magnetizations in the Salé core.

Age Model

The data from the B series samples were converted from depth to age by linearly interpolating between the datum levels listed in Table 1. The ages assigned to polarity reversals are those suggested by S. C. Cande and D. V. Kent (Revised calibration of the geomagnetic polarity timescale for the late Cretaceous and Cenozoic, submitted to *Journal of Geophysical Research*, 1994 (hereinafter referred to as submitted manuscript, 1994)) who recalibrated the distances between anomalies of *Cande and Kent* [1992] using a date of 5.23 Ma for the base of the Thvera (Subchorn C3n.4n) from the astronomical timescale of *Hilgen* [1991a] as the youngest calibration tie point for interpolation. These ages are similar to those calculated by *Shackleton et al.* [1994b] who used a date of 5.875 Ma for the top of C3An.1n (top) and 9.639 Ma for the top of C5n.1n [*Baksi*, 1993] (Table 1). Chronologic control in the S series samples is poor because there are no biostratigraphic or polarity reversal events in the top of the section (Figure 4). Because of this inadequate stratigraphic control, we have chosen not to convert the S series samples to a timescale and present these results versus depth only.

Time Series Analysis

We have considerable confidence in the paleomagnetically controlled age model for the B-series samples. For the interval from the top of Chron C3Bn to the top of C3An (6.935 to 5.894 Ma), we utilized standard time series analysis techniques to estimate the power spectral density as a function of frequency for the isotope and carbonate signals [*Jenkins and Watts*, 1968]. The timeseries data were interpolated at uniform 5 kyr intervals and the resulting signals were linearly detrended, a prewhitening constant of 0.5 was applied to the isotope analysis to suppress low-frequency peaks, no prewhitening was applied to the carbonate signal, and all estimates were made with 1/3 lag. The power spectrum (log variance versus frequency) for the oxygen isotope signal reveals a significant peak at 40 kyr (Figure 9a), which correspond to the Milankovitch cycles of obliquity (41 kyr). The power spectrum for the carbonate signal displays a significant peak at 100 kyr (Figure 9b), which corresponds to the

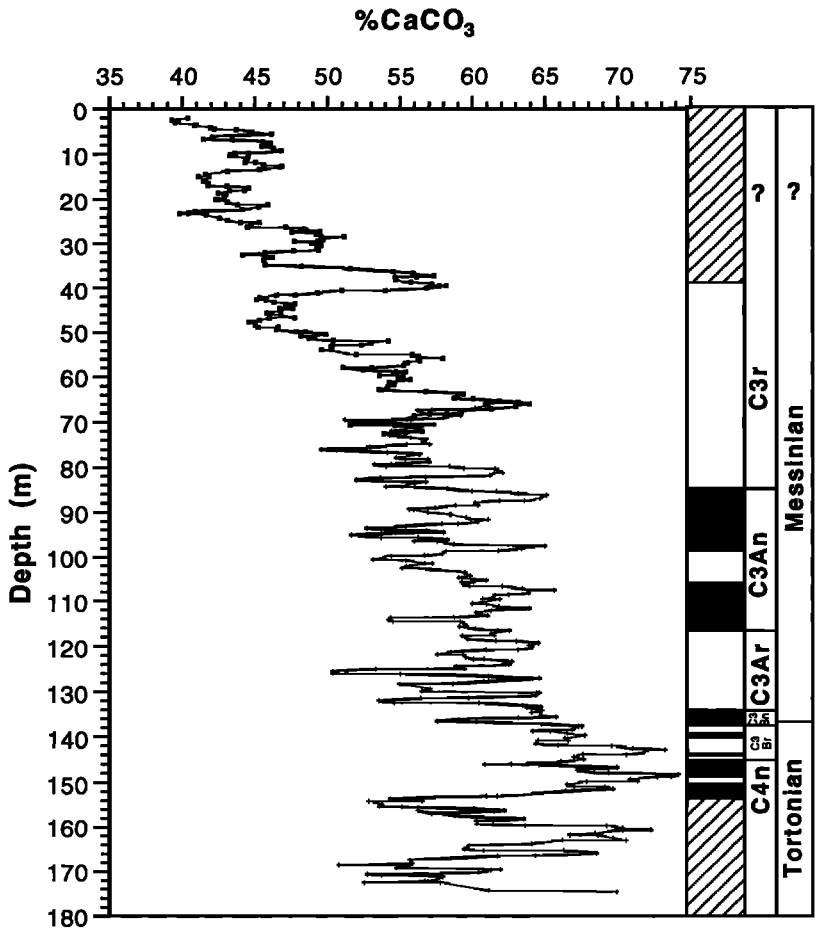

Figure 7. Three-point running average of the percent carbonate results of the B series (crosses) and S series (squares) samples from the Salé core. Note the distinct trend toward lower $\%CaCO_3$ values toward the top of the core.

Milankovitch cycle of eccentricity (100 kyr). No significant power was detected at precessional periods (23 and 19 kyrs) in either record, probably because the sampling interval is close to or less than the Nyquist frequency for precession.

Oxygen Isotope Stage Nomenclature

Oxygen isotopes have provided paleoceanographers with a stratigraphic tool that makes correlation possible to within a few thousand years during the past 2.5 m.y. [*Imbrie et al.*, 1984; *Ruddiman et al.*, 1989; *Raymo et al.*, 1989]. *Shackleton et al.* [1994a] have extended oxygen isotope stratigraphy into the latest Miocene by developing a stage numbering scheme using the benthic oxygen isotope record from site 846 in the eastern equatorial Pacific. The oldest stage identified was TG24 in the oldest reversed subchron of the Gilbert (Chron C3r). "TG" stands for the time period below the base of the Thvera Subchron to the base of the Gilbert (equivalent to Chron C3r). Beyond Stage TG24 the oxygen isotope record at site 846 was marked by low-amplitude variation which made it difficult to recognize distinct stages. In this study we begin where the isotope stage nomenclature of *Shackleton et al.* [1994a] leaves off in Chron C3r and identify stages to the top of C3Bn (6.935 Ma).

We follow the isotope stage nomenclature of *Shackleton et al.* [1994], who adopted the scheme of *Hays et al.* [1969] used for Pacific carbonate cycles. By this method the numbering of isotope and carbonate stages restarts at each major polarity reversal boundary. For chrons beginning with C3An we suggest limiting the numbering to polarity intervals which are robust compared to some of the minor subchrons. For example, the stage nomenclature would become cumbersome if numbering were to re-start at each of the subchrons of C3An. Consequently, we suggest re-initializing the numbering of stages at the top of C3An and C3Ar only.

The oxygen isotope signal shows clear evidence of 41-kyr cycles during Chrons C3An and C3Ar (Figures 9a and 10). Chron C3Ar spans the interval between 6.935 and 6.137 Ma, a duration of 368,000 years. During this interval, 18 stages were identified and designated C3Ar.δ^{18}O.1 through C3Ar.δ^{18}O.18 in accord with the nomenclature of *Shackleton et al.* [1994a] (Figure 10). Chron C3An spans the time from 6.567 to 5.894 Ma, a duration of 673,000 years. During this interval, 34 stages have been identified and designated C3An.δ^{18}O.1 through C3An.δ^{18}O.34 (Figure 10).

The most distinctive feature of the oxygen isotope record during Chron C3r are two pronounced glacial stages (TG20 and

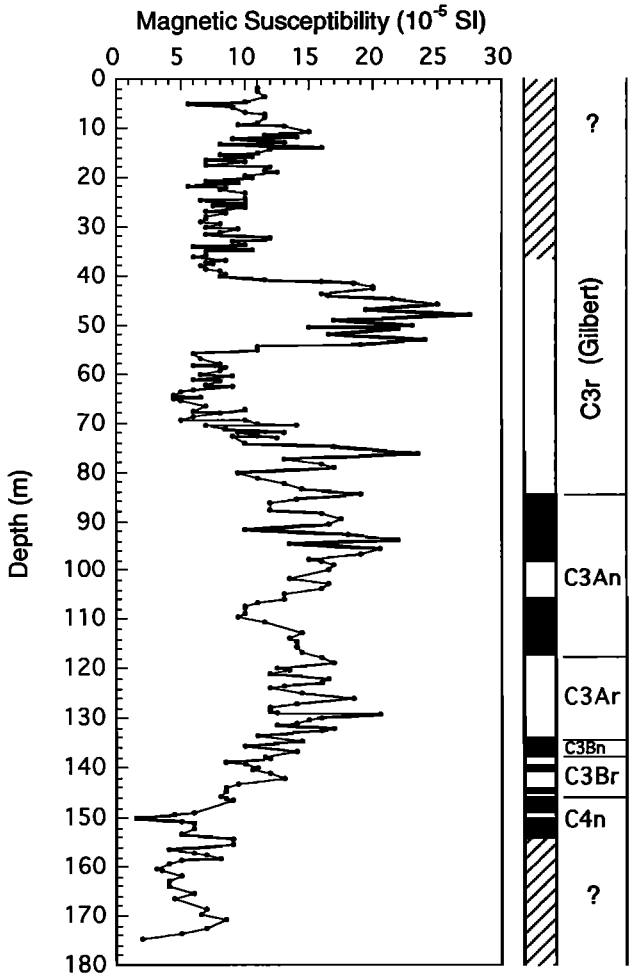

Figure 8. Initial magnetic susceptibility of B and S series samples from the Salé core. Intervals of weak susceptibility, especially between 0-40 m and 154-175 m, generally correspond to a poor paleomagnetic record with the rejection of many samples on the basis of weak, unstable magnetization. Conversely, invervals of high susceptibility gave better paleomagnetic results with few samples rejected. Note the overall poor relationship of susceptibility to the $\%CaCO_3$ record shown in Figure 7.

22) that are recognized in both the S and B-series samples because of the overlap between the cores (Figures 10 and 11). The oldest stage identified by *Shackleton et al.* [1994a] was TG24. In the B series samples the amplitude of the $\delta^{18}O$ signal is low from stage TG22 to the Chron C3r/C3An boundary, but distinct glacial-to-interglacial cycles can be deciphered from this interval (Figure 10). We propose to extend the isotope taxonomy of *Shackleton et al.* [1994a] to the top of Chron C3An by the addition of 10 stages designated TG25 through TG34 (Figure 10). If the 41 kyr cycles observed for oxygen isotopic variation during Chrons C3An and C3Ar (Figure 9a) can be extrapolated to Chron C3r, then we estimate an age of 5.63 Ma for stage TG22, which is 130 kyr younger than the age of 5.76 Ma estimated by *Shackleton et al.* [1994a]. They regarded the timescale for site 846 as suspect in detail for the interval between 5 and 6 Ma, because of low coherencies between the GRAPE (gamma ray attenuation porosity evaluator) record at site 846 and the stacked GRAPE record that was used to construct the timescale [*Shackleton et al.*, 1994b]. Additionally, no concentration of power at orbital frequencies was found in the oxygen isotope record during this interval [*Shackleton et al.*, 1994a].

Above stage TG20, the next most pronounced glacial stages are TG14 and TG12, which are recognized in the Salé record (Figure 11). *Shackleton et al.* [1994a] identified 5 stages between TG14 and TG20, whereas the Salé record suggests seven distinct stages (Figure 11). In the Salé record we tentatively identify stages TG11, 10, and 9, but we are uncertain how to correlate stages above this level. A series of high-amplitude fluctuations between 10 and 30 m may correlate to stages T2 to T8 in the Thvera Subchron (Figure 11), but it is not clear how the isotope stages then correlate between T8 and TG9. Either the Salé record is compressed in this interval or the site 846 record has been expanded because of an error in age assignment. The lack of adequate paleomagnetic or biostratigraphic control in the Salé core above 40 m reduces confidence in any stage identifications for this interval.

Discussion

The detailed carbonate, stable isotope, and magnetostratigrahic records from the Salé core permit us to frame the historical events that occurred during the Tortonian and Messinian stages into a precise chronologic framework using the timescale of *Cande and Kent* [1992, submitted manuscript, 1994]. Many attempts have been made to correlate the events of the Messinian salinity crisis to oxygen isotope and eustatic records [*Ryan et al.*, 1974; *Adams et al.*, 1977; *McKenzie and Oberhansli*, 1985; *Cita and McKenzie*, 1986; *Hodell et al.*, 1986; *Hodell and Kennett*, 1986; *Müller and Hsü*, 1987; *Hodell et al.*, 1989; *Kastens*, 1992; *Rouchy and St. Martin*, 1992; *Aharon et al.*, 1993; among others]. These correlations have often been speculative and tenuous because of the poor magnetobiostratigraphic control within the Mediterranean, especially during the time of evaporite deposition. We focus here on the time leading up to the salinity crisis when open marine, or partially restricted, conditions prevailed in the Mediterranean and when magnetobiostratigraphic information is reasonably good.

The Tortonian Stage

The Tortonian stage in the Mediterranean was marked by open marine conditions and the normal deposition of "blue marls" in Sicily [*Thunell et al.*, 1987]. In the Salé core, this interval was characterized by relatively low benthic foraminiferal $\delta^{18}O$ values (Figure 5), high $\delta^{13}C$ values (Figure 6), and high carbonate content (Figure 7). During the latest Tortonian, the oxygen isotopic signal shows a brief period of minimum $\delta^{18}O$ beginning at the base of C4n.1n (7.562 Ma) and continuing into C3Br.2r (~7.2 Ma; Figure 5). We correlate this event to a similar decrease observed in the oxygen isotopic record from DSDP site 588 in the southwest Pacific (designated Event F by *Hodell and Kennett* [1986]), which was interpreted as indicating an interval of climatic warmth or deglaciation. This event is also marked by relatively high $\delta^{13}C$ and carbonate values and immediately precedes the start of the late Miocene carbon isotope shift (Figure 6 and 7).

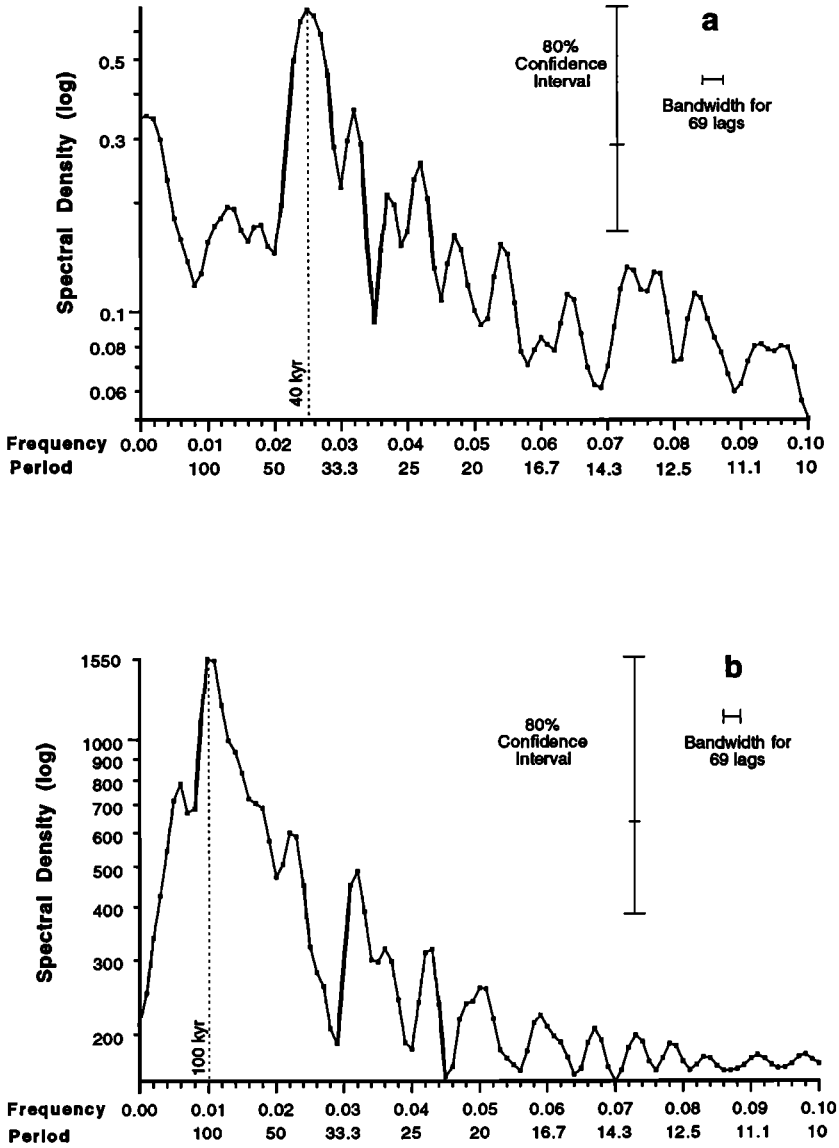

Figure 9. Power spectrum (log variance versus frequency) for (a) the oxygen isotope and (b) carbonate signals during Chrons C3An and C3Ar (5.894 to 6.935 Ma). Note the power concentrated at periods of 40-kyr in the isotope signal (Figure 9a) and 100-kyr in the carbonate signal (Figure 9b). These periods correspond to the Milankovitch cycles of orbital obliquity (41 kyr) and eccentricity (100 kyr), respectively.

The Tortonian/Messinian Boundary

Near the Tortonian/Messinian boundary in the Salé core a number of pronounced isotopic and faunal changes occurred including: (1) a 1‰ decrease in benthic foraminiferal $\delta^{13}C$ values (Figure 6); (2) a mean increase of 0.4‰ in benthic foraminiferal $\delta^{18}O$ values (Figure 5); (3) a shift in planktonic foraminifera from an assemblage dominated by *Globorotalia menardii* to an assemblage consisting of the *Globorotalia miotumida* plexus and globoconeliids (Figure 4); and (4) the sudden appearance of upper psychrospheric ostracodes such as *Agrenocythere pliocenica* (Figure 4). These same events have been recognized by us previously in other nearby sequences in Morocco [*Hodell et al.*, 1989; *Benson et al.*, 1991; *Benson and Rakic-El Bied*, 1991a].

The Late Miocene Carbon Isotope Shift

Much has been written about the global decrease in the $\delta^{13}C$ of oceanic dissolved inorganic carbon (DIC) that occurred during the late Miocene since its discovery by *Keigwin and Shackleton* [1980]. In the Salé core, $\delta^{13}C$ values continuously decreased between 7.6 and 6.8 Ma (Figure 12), but this is largely due to the maximum in $\delta^{13}C$ values that occurred during Chron C4n. When the entire $\delta^{13}C$ record is considered, the decrease in mean $\delta^{13}C$ values began near the base of Chron C3Bn (7.1 Ma) and ended in Chron C3Ar (~6.8 Ma) (Figure 6). Just following the carbon shift, there are a series of highly depleted $\delta^{13}C$ values in Chron C3Ar. One or more of these minima have been reported in other carbon isotopic records (e.g., site 588) [*Hodell and Kennett*, 1986].

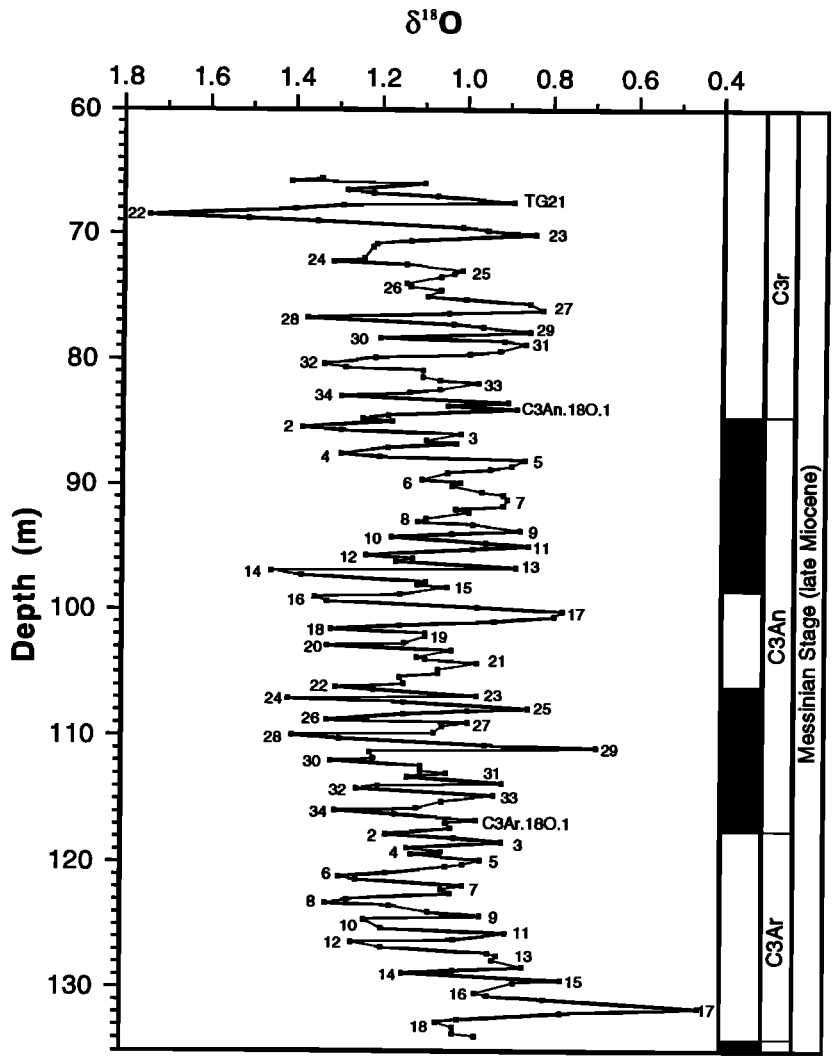

Figure 10. Oxygen isotopic results of the benthic foraminifera, *Planulina ariminensis*, for the B series samples from the base of Chron C3Ar to Chron C3r. Isotopic stages beyond TG24 represent an extension of the oxygen isotopic stage nomenclature of *Shackleton et al.* [1994a]. The prefix of the stage numbering changes just above the top of C3An and C3Ar so that the first stage is odd and corresponds to an interglaciation. We've identified 34 stages during Chron C3An and 18 stages during Chron C3Ar.

Because the decrease in $\delta^{13}C$ is observed in both planktic and benthic records in all ocean basins, the carbon shift must partly represent either a decrease in the $\delta^{13}C$ of dissolved riverine bicarbonate or a decrease in the fraction of carbon removed from the ocean by organic carbon versus carbonate carbon. Many authors have proposed that the carbon shift resulted from the increased erosion of organic carbon from terrigenous soils and shelf sediments during a drop in sea level as a result of Antarctic glaciation [*Vincent et al.*, 1980; *Loutit and Keigwin*, 1982; *Berger and Vincent*, 1986]. In the Salé core the decrease in benthic foraminiferal $\delta^{13}C$ values coincides with an increase in $\delta^{18}O$ values (Figure 12), which is compatible with the association of ice volume increase at the time of the carbon shift, but does not prove the point conclusively. This relationship has not been found in all cores, however, and some isotopic records show no evidence for increased glaciation at the time of the carbon shift [*Keigwin*, 1987; *Müller et al.*, 1991].

Recent findings of a change in the carbon isotope composition of paleosol carbonate nodules between 6 and 7 Ma may be related to the oceanic carbon shift during the late Miocene [*Cerling et al.*, 1989; *Quade et al.*, 1989]. This change in terrestrial $\delta^{13}C$ is opposite in direction to the oceanic carbon shift and has been interpreted as reflecting a shift from C_3-dominated to C_4-dominated ecosystems. This shift from C_3 to C_4 ecosystems was also accompanied by an overall decrease in global biomass, which may have caused the marine decrease in $\delta^{13}C$ values during the late Miocene. A net transfer of carbon from the terrestrial (land plants and soils) to the oceanic reservoir could explain the carbon shift. By tabulation of benthic foraminiferal $\delta^{13}C$ data from over 25 cores throughout the oceans, the average shift in oceanic $\delta^{13}C$ of DIC was about 0.5‰. Assuming an oceanic mass of carbon of 38,000 gT [*Schlesinger*, 1991] and an average $\delta^{13}C$ of C_3 organic carbon of -25‰, the carbon shift could be explained by the transfer of 950 gT of organic carbon from the terrestrial reservoir

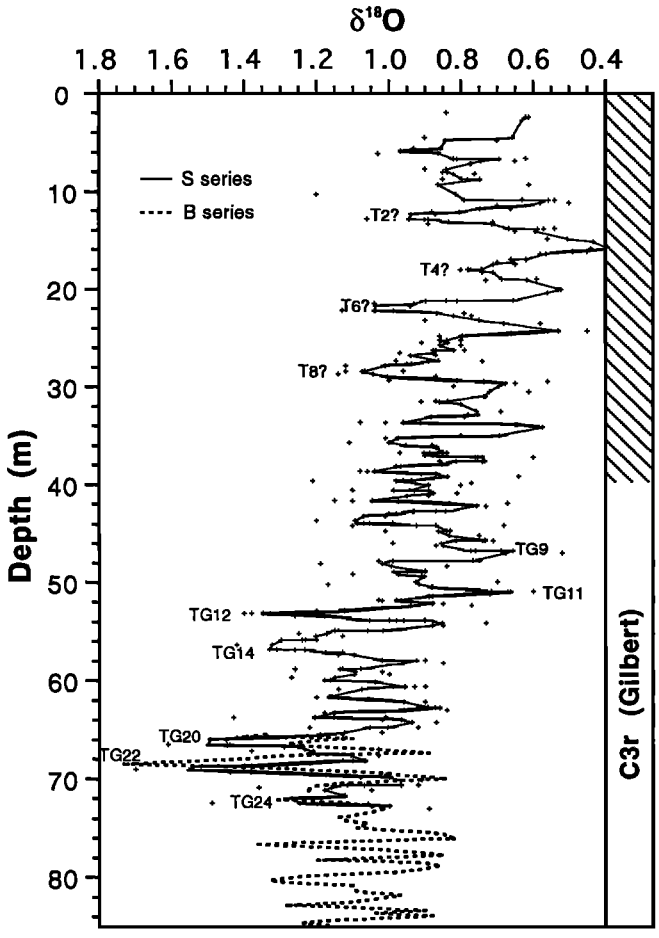

Figure 11. Oxygen isotopic results of the benthic foraminifera, *Planulina ariminensis*, in the B series (dashed line) and S series (solid line) samples for the time interval younger than 5.894 Ma (top of Chron C3An). The line connecting the S series data is a 3-point running mean of individual data points shown by crosses. Oxygen isotopes stages are those identified by *Shackleton et al.* [1994a] at ODP site 846 in the eastern equatorial Pacific. Questionable stages are indicated by a question mark.

to the oceanic reservoir. Today, the terrestrial carbon reservoir contains a total of 2060 gT of carbon including both land plants (560 gT) and soil carbon (1500 gT) [*Schlesinger*, 1991]. This indicates that the terrestrial carbon pool may have been about 1.4 times larger than present before the carbon shift and shrank by about 30% between ~7.1 and 6.8 Ma.

Because C_4 plants represent an adaptation to water stress, the expansion of grassland habitats and C_4 plants between 6 and 7 Ma may have been related to increased aridity. Increased aridity in the Mediterranean region may have contributed to the onset of a negative water budget in the Mediterranean near the Tortonian/Messinian boundary [*Hodell et al.*, 1989; *Benson et al.*, 1991]. Indeed, palynological evidence indicates a change toward drier climate during the late Miocene, which may have predisposed the Mediterranean to desiccation [*Suc*, 1986, 1989; *Suc and Bessais*, 1990].

It has been proposed that the increase in $\delta^{13}C$ of pedogenic carbonates during the late Miocene may have been related to a decrease in atmospheric pCO_2 from 800 to 400 ppmV [*Retallack*, 1993]. Such a decrease in CO_2 may have resulted in global cooling, expansion of polar ice caps, and the onset of the Messinian salinity crisis [*Retallack*, 1993]. Although our isotope data from Salé cannot prove this to be the case, the observed relationships among the late Miocene carbon shift, increase in $\delta^{18}O$ values, and onset of a negative water budget in the Mediterranean are consistent with such a scenario [*Hodell et al.*, 1989; *Benson et al.*, 1991]. A large body of microfossil evidence also supports substantial climatic cooling during the late Miocene [*Ingle*, 1967; *Kennett*, 1967; *Wolfe and Hopkins*, 1967; *Barron and Keller*, 1983; *Kennett and Vella*, 1975; *Kennett and Watkins*, 1974; *Hodell and Kennett*, 1986]. To test whether atmospheric CO_2 levels declined significantly during the late Miocene and led to global cooling, measurements of the $\delta^{13}C$ of organic carbon, a potential proxy for pCO_2 [*Rau et al.*, 1989; *Freeman and Hayes*, 1992], need to be made during the late Miocene.

Oxygen Isotopes, Glacial Eustacy, and the Onset of "Crisis Conditions" in the Mediterranean

The Salé record shows a distinct increase in mean $\delta^{18}O$ values across the Tortonian/Messinian boundary (Figures 5 and 12). This increase in oxygen isotopic ratios has been reported previously from nearby Moroccan sections [*Hodell et al.*, 1989] and interpreted to represent decreased temperature and/or increased continental ice volume. The $\delta^{18}O$ signal in the Salé core indicates that the increase occurred in two steps. The first step occurred at 7.17 Ma at the base of C3Br.1n, and a second increase occurred at ~6.8 Ma in Chron C3Ar (Figure 12). The older increase in $\delta^{18}O$ values coincides with the sudden appearance of upper psychrospheric ostracods (*Agrenocythere pliocenica*) in the Salé core (Figure 4) [*Hodell et al.*, 1989; *Benson et al.*, 1991]. This event has been interpreted as reflecting a reversal in deep water flow through the Rifian Corridor, whereby warm waters of Mediterranean origin were replaced by cold intermediate waters of Atlantic origin [*Hodell et al.*, 1989; *Benson et al.*, 1991]. The current reversal within the Rifian Corridor marks the establishment of a strong negative water balance in the Mediterranean and the onset of restricted circulation with the Atlantic [*Hodell et al.*, 1989; *Benson et al.*, 1991]. We proposed previously that the reversal in deepwater circulation at this time resulted in the inflow of nutrient-rich Atlantic intermediate water into the Mediterranean, which stimulated productivity and resulted in the deposition of organic-rich strata, reefs, and diatomites [*Hodell et al.*, 1989; *Benson et al.*, 1991; *Cunningham et al.*, 1994].

It is possible to correlate the record of the Salé drill core with ODP site 654 in the Tyrrhenian Sea, which recovered the first deep-sea record that contains a history of the initiation of the Messinian salinity crisis [*Kastens and Mascle*, 1990]. Two magnetostratigraphic interpretations have been proposed for site 654 [*Kastens*, 1992], but biostratigraphic correlations between site 654 and Morocco strongly supports Interpretation A of *Channell et al.* [1990b]. In this interpretation the replacement of the *Globorotalia menardii* group by the *Globorotalia miotumida* group (PF-Event 3) [*Sierro*, 1985] and the FCO of *G. conomiozea* both occur in Chron C3Bn [*Glacon et al.*, 1990], as they do at Salé (Figure 4) and other Moroccan sections [*Moreau et al.*, 1985/86; *Hodell et al.*, 1989; *Benson et al.*, 1991; *Benson and Rakic-El Bied*, 1991a].

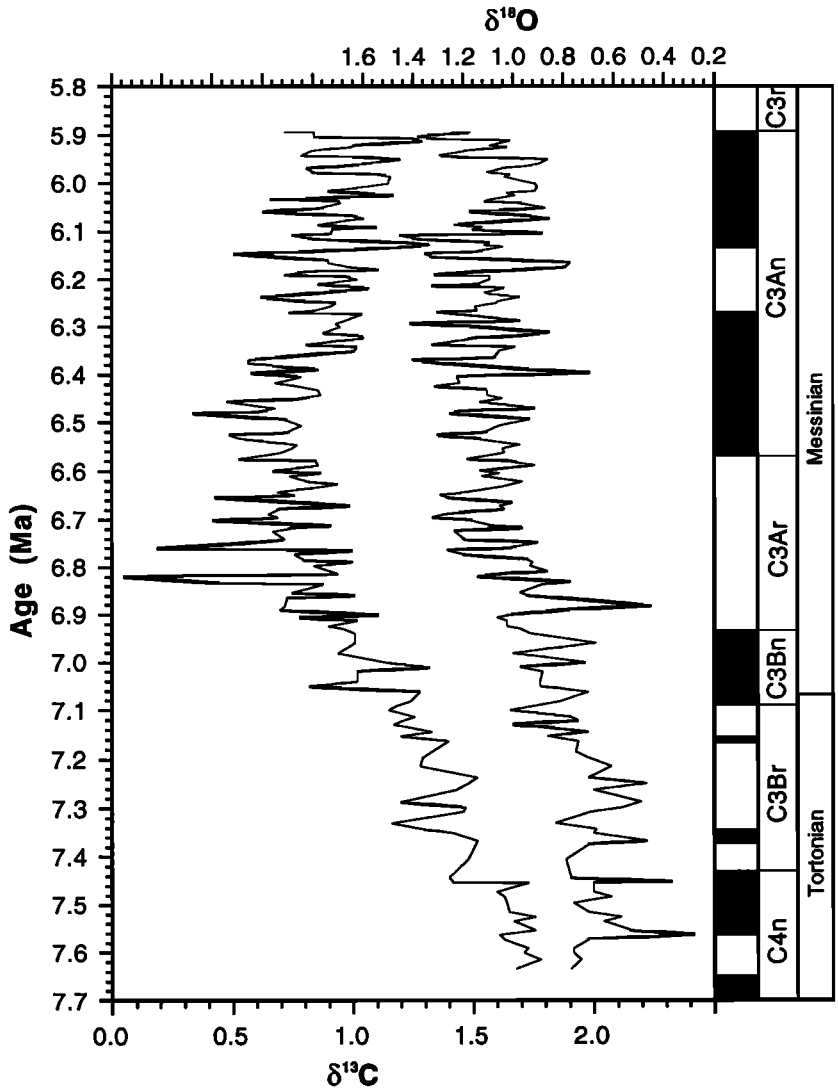

Figure 12 Stable isotopes of (left) carbon and (right) oxygen of the benthic foraminifera, *Planulina ariminensis*, from the B series samples of the Salé relative to the timescale of *Cande and Kent* [1992, submitted manuscript 1994].

The first lithologic sign of the impending salinity crisis at Site 654 occurs at 348.9 mbsf (meters below seafloor) at the base of lithologic unit III, which is composed of dark-colored, finely laminated, dolomitic, organic-rich sediments containing radiolarians, sponge spicules, and diatoms [*Kastens and Mascle*, 1990]. This unit is considered to be equivalent to the Tripoli Foramtion [*Borsetti et al.*, 1990], exposed in Sicily, which also consists of cyclic alternations of organic-rich diatomites and claystones and marks the onset of "crisis conditions" in the Mediterranean [*McKenzie et al.*, 1979/1980]. The base of unit III in site 654 occurs at 348.9 mbsf, which is 8.4 m above a change from normal to reversed polarity located at 357.34 m and interpreted as the top of Chron C3Bn (6.935 Ma) [*Channell et al.*, 1990b]. In the stratotype section at Falconara, Sicily, the Tripoli Formation begins some 5 to 8 m above the Tortonian/Messinian boundary as recognized by the FCO of *G. conomiozea* [*Colalongo et al.*, 1979; *Benson et al.*, 1991]. Direct paleomagnetic dating of the base of the Tripoli is not possible at Falconara because the entire section has been remagnetized [*Langereis and Dekkers*, 1992].

We suggest that the increase in $\delta^{18}O$ values at 6.8 Ma in the Salé core correlates to the base of the Tripoli Formation and the first evidence of crisis conditions in site 654 and Sicilian sections. Support for this comes from *Glacon et al.* [1990] who found an increase in $\delta^{18}O$ values in early Messinian marls in site 654, suggesting that net evaporation had increased in the Mediterranean before the lithologic change observed at the base of Unit III [*Kastens and Mascle*, 1990]. Anomalously high $\delta^{18}O$ values of dolomites in Unit III of site 654 also suggest a high degree of evaporation in the waters where dolomite crystallization occurred [*Pierre and Rouchy*, 1990]. Similarly, *McKenzie et al.* [1979/1980] also reported high $\delta^{18}O$ values of dolomites from the Tripoli Formation in Sicily which were interpreted to reflect highly evaporative conditions during sea level lowstands.

A long-standing controversy has ensued regarding glacio-eustatic versus tectonic causes for the isolation of the

Mediterranean during the Messinian (see *Kastens* [1992] for a review). *Shackleton and Kennett* [1975] originally proposed that the Antarctic ice sheet increased to 1.5 times its present volume during the late Miocene on the basis of an increase in $\delta^{18}O$ values of DSDP site 284 (see also *Hodell and Kennett* [1986]). Some sites show a similar increase in mean $\delta^{18}O$ values during the late Miocene (e.g., site 519 and CH115) [*Hodell et al.*, 1986]; *Hodell and Kennett* [1986]), whereas other sites do not (e.g., sites 588 and 552) [*Hodell and Kennett*, 1986; *Keigwin*, 1987]). The isotopic "smoking gun" for increased glaciation coinciding with the onset of the Messinian Salinity Crisis has been elusive [*Kastens*, 1992]. The benthic foraminiferal $\delta^{18}O$ signal from Salé leaves little doubt that a two-step increase in $\delta^{18}O$ values occurred at 7.17 and 6.8 Ma (Figure 12). The latter appears to correlate to the onset of restricted circulation in the Mediterranean. The pertinent question is whether this increase in $\delta^{18}O$ values represents a local cooling of deep waters in the Rifian Corridor or does it also reflect increased continental ice volume. We suggest that the increase in $\delta^{18}O$ values during the late Miocene represents, at least in part, an increase in global ice volume that lowered sea level and contributed to the establishment of a negative water budget in the Mediterranean.

Ample ancillary evidence exists for global cooling and increased Antarctic ice volume during the late Miocene and the reader is referred to *Hodell and Kennett* [1986] for a review of the older literature. Recent drilling in the southern ocean supports previous evidence of a major cooling episode and pulses of ice sheet expansion on Antarctica during the latest Miocene [*Kennett and Barker*, 1990; *Müller et al.*, 1991; *Ehrmann et al.*, 1992]. Drilling results from the Greenland margin indicate that the oldest glaciomarine sediments are 7.0 m.y. old, suggesting that initial growth of northern hemisphere ice caps also began during the late Miocene [*Larsen et al.*, 1994]. Low concentrations of fine-grained IRD have also been reported from the Norwegian Sea from sediments as old as the late Miocene [*Jansen and Sjoholm*, 1991].

A late Miocene regressive phase is commonly found in sedimentary sequences throughout the world [*Adams et al.*, 1977]. Sequence stratigraphy [*Haq et al.*, 1987] has identified two important falls in sea level at ~6.3 and 5.5 Ma in the late Miocene (timescale of *Berggren et al.* [1985]), which is equivalent to ~6.8 and 6.1 Ma on the timescale of *Cande and Kent* [1992, submitted manuscript, 1994]. In a study of sea level changes from the Niue Atoll, South Pacific, *Aharon et al.* [1993] found evidence for sealevel changes of about 10 m amplitude beginning at 6.14 Ma reaching an amplitude of at least 30 m at 5.26 Ma (time scale of *Hilgen* [1991a], which is the same as Cande and Kent (submitted manuscript, 1994).

We conclude that together with the trend of longterm tectonic compression in the Betic-Rif Orogen, glacio-eustatic lowering of sea level near the Tortonian/Messinian boundary contributed to the onset of a negative water budget for the Mediterranean and the reversal in deepwater flow through the Rifian Corridor [*Hodell et al.*, 1989; *Benson et al.*, 1991]. We correlate the $\delta^{18}O$ increase at 6.8 Ma at Salé to the base of the Tripoli Formation and the beginning of crisis conditions in the Mediterranean, although evaporite deposition did not begin until much later.

The Messinian Evaporites

In Sicily, the top of the Tripoli diatomites is overlain by the Calcare di Base, which represents an evaporitic limestone facies that heralds the onset of evaporite deposition [*McKenzie et al.*, 1979/1980; *Pedley and Grasso*, 1993]. The top of the Tripoli Formation occurs near a change in the coiling direction of *N. acostaensis* (PF-Event 4 of *Sierro et al.* [1993]) . In the Salé core the first in a series of coiling changes in *N. acostaensis* begins at 102.1 m during Subchron C3An.1r (Figure 4). We have proposed previously that this level occurs just below the base of the Calcare di Base and that the onset of deposition of the lower evaporites probably began in C3An.1n [*Hodell et al.*, 1989; *Benson and Rakic-El Bied*, 1991a]. *Gautier et al.* [1994] have suggested that there may be a significant hiatus at Falconara between the top of the Tripoli and the base of the Calcare di Base. They proposed that evaporite deposition did not begin in the Mediterranean until early Chron C3r at ~5.7 Ma, and the entire salinity crisis was limited to Chron C3r between 5.7 and 5.3 Ma. In site 654, balatino gypsums belonging to the upper evaporites were assinged to Chron C3r [*Channell et al.*, 1990b], but the history of any older evaporite deposition in Chron C3An is probably missing in one or more hiatuses within lithostratigrahic units II and III [*Kastens*, 1992]. Alternatively, Interpretation B of the polarity reversal stratigraphy of site 654 would also place the entire salinity crisis in C3r [*Kastens*, 1992] in accord with *Gautier et al.* [1994].

During the Messinian the magnitude of oxygen isotope values during glacial stages are fairly uniform with the exception of glacial stages TG22 and TG20 during early Chron C3r (Figures 10 and 11). These were the two strongest glacial stages of the entire Messinian. *Shackleton et al.* [1994a] suggested that the major glaciations represented by these stages in Chron C3r may have been responsible for the complete isolation of the Mediterranean from the world ocean. Support for this interpretation comes from the dating of a major exposure surface at the top of the terminal carbonate complex (TCC) in the Melilla Basin (eastern Morocco), which marks a transition from marine to continental deposits [*Cunningham et al.*, 1994]. The TCC has been dated using $^{40}Ar/^{39}Ar$ to 5.83 Ma [*Cunningham et al.*, 1994], which correlates to earliest Chron C3r just below stage TG22. The estimated magnitude of sea level fall at the base of TG22 is of the order of 50 m [*Shackleton et al.*, 1994a]. This event may also be associated with a major dissolution unconformity just below the Miocene/Pliocene boundary on atolls in the Pacific where the magnitude of sea level fall was estimated to be at least 30 m [*Aïssaoui and Kirschvink*, 1991; *Aharons et al.*, 1993]. Maximum $\delta^{18}O$ values associated with stage TG22 and 20 during Chron C3r are common features of oxygen isotope records, although only one of the two events may be present or they may be combined in low resolution records (e.g., site 588 [*Hodell and Kennett*, 1986]; site 552 [*Keigwin*, 1987]; site 519 [*McKenzie and Oberhansli*, 1985]).

Milankovitch Cyclicity During the Messinian

The Salé drill core shows distinct glacial-to-interglacial changes in $\delta^{18}O$ during the Messinian with a range in $\delta^{18}O$ values of 0.5 to 0.6‰ or about 1/3 the signal of the late Pleistocene (Figure 11). Spectral analysis of the $\delta^{18}O$ record between 6.935 and 5.78 Ma shows that the signal is dominated by power at 40 kyr (Figure 10a), which is close to the 41-kyr cycle of orbital obliquity. The concentration of power near the obliquity period suggests that the $\delta^{18}O$ signal was partly controlled by changes in continental ice volume that were responding to insolation changes at high latitude. With the exception of the interval from 5 to 6

Ma, *Shackleton et al.* [1994a] have shown significant coherency between $\delta^{18}O$ and insolation in the obliquity band for the Pliocene between 1.7 and 5 Ma. The Salé oxygen isotope record indicates that the Messinian Stage was also marked by the waxing and waning of icesheets with a period of 41 kyr. We consider Antarctica to be the most likely source of this ice volume variation, but growth and decay of ice caps and small icesheets in the northern hemisphere may have also contributed to the $\delta^{18}O$ variation [*Larsen et al.*, 1994].

Cyclicity in the carbonate record is dominated by the eccentricity cycle of 100 kyrs and no significant power was detected at precessional periods (Figure 10b). We interpret the 100-kyr carbonate signal as representing the long-term modulation of the precession cycle by eccentricity. We suspect that the precessional peak is absent from the carbonate power spectrum because the sampling interval for the carbonate record is greater than the Nyquist frequency for precession. Precessional forcing exerts the strongest influence on climate at 35°N where the obliquity signal is suppressed. Indeed, precessional forcing appears to have dominated the Plio-Pleistocene sediment record in the Mediterranean [*Hilgen*, 1987, 1991a, b] and evidence of precessional forcing has also been found in the late Miocene [*Krijgsman et al.*, 1994] (R.-H. Benson, L.C. Hayek, D.A. Hodell, and K. Rakic-El Bied, Extending the climatic precession curve back into the Miocene by signature template comparison, and the consequences of "solar pumping" on the Messinian salinity crisis, submitted to *Paleoceanography*, 1994 (hereinafter referred to as submitted manuscript, 1994)).

Variations in Antarctic ice volume have been called upon to explain the fluctuations in sea level that controlled marine inundations into the Mediterranean during the Messinian. For example, *McKenzie et al.* [1979/1980] proposed that the Tripoli diatomites were deposited under normal marine conditions during transgressions, whereas sea level lowstands resulted in restricted circulation which favored the formation of dolomitizing solutions that diagenetically altered the carbonates in the clay-rich sediments. Faunal and sediment cyclicity is pervasive in the Tripoli Formation and overlying Calcare di Base [*Pedley and Grasso*, 1993]. The evaporites also show evidence of cyclic deposition and it has been argued that the large volume of evaporites deposited in the Mediterranean require multiple cycles of marine refill and drawdown.

The oxygen isotopic record from Salé cannot be used to prove or disprove the existence or number of marine inundations during the salinity crisis, because this evidence must come from within the Mediterranean itself. We simply wish to point out that high-frequency variations in $\delta^{18}O$ (and presumably Antarctic ice volume) were occurring throughout the time represented by the Messinian evaporites and it is possible, then, that marine inundations occurred during interglacial stages during this interval. The oxygen isotopic stages defined in Figure 11 provide a template against which intra-Messinian cycles can be compared once they have been properly enumerated within the Mediterranean.

The Zanclean Deluge

The Miocene/Pliocene boundary is associated with the return of open marine conditions to the Mediterranean after the salinity crisis [*Cita*, 1975], and has been dated at 5.32 Ma by counting five 21-kyr precessional cycles (or 105 kyr) below the base of the Thvera subchron in the Eraclea Minoa section, Sicily [*Hilgen and Langereis*, 1993]. Both tectonic and eustatic causes have been proposed to explain the sudden change from the "Lago Mare" conditions near the end of the Messinian to the open marine conditions at the base of the Zanclean. Many authors have suggested a relationship between decreasing $\delta^{18}O$ values, Antarctic deglaciation, marine transgression, reflooding of the Mediterranean, and termination of the salinity crisis [*McKenzie and Oberhansli*, 1985; *Hodell et al.*, 1986; *Hodell and Kennett*, 1986; *McKenzie and Sprovieri*, 1990; *Kastens*, 1992].

The oxygen isotopic record at Salé contains a distinct decrease in $\delta^{18}O$ values at the transition from stage TG12 to TG11 (Figure 11). Following this event, $\delta^{18}O$ minima became progressively more intense indicating less ice volume and/or warmer temperatures during interglacial periods of Chron C3r. Mean oxygen isotope values near the top of the Salé core are as low as those from the bottom of the core during the Tortonian, when open marine conditions prevailed in the Mediterranean prior to the salinity crisis (Figure 5). In site 846, *Shackleton et al.* [1994a] also documented a trend of decreasing $\delta^{18}O$ values during Chron C3r, culminating in the most depleted $\delta^{18}O$ values during stage TG9 at ~5.46 Ma. Because this age is 140,000 years older than the Miocene/Pliocene boundary, they concluded that the correlation between extreme interglacial episodes and the base of the Trubi marls (marking the Zanclean Deluge) may be incorrect. According to their chronology, the Miocene/Pliocene boundary is correlated to stage TG5 which displays relatively light $\delta^{18}O$ values but does not stand out as being an extreme interglacial event.

By extrapolation of the 41-kyr oxygen isotopic cycles at Salé, we estimate an age of 5.63 Ma for stage TG22, which is 130 kyr younger than that estimated in site 846. Carrying this exercise further upsection, we estimate the ages for the following isotope stages: TG20 (5.562 Ma), TG14 (5.398 Ma), TG12 (5.357 Ma), and TG10 (5.316 Ma). If these age estimates are correct, then the Miocene/Pliocene boundary (5.32 Ma) would occur in stage TG11 at the sharp decrease in $\delta^{18}O$ values (Figure 11). This result is consistent with scenarios that invoke a rise in sea level as the cause of the flooding of the Mediterranean and termination of the salinity crisis. We emphasize, however, that our age control is poor in the S series samples and this conclusion is entirely contingent upon the correct identification and extrapolation of 41-kyr oxygen isotope cycles into Chron C3r (Figure 11). Other high-resolution $\delta^{18}O$ records with better time control during Chron C3r are needed to test the relationship between global ice volume changes and the termination of the Messinian salinity crisis at the Miocene/Pliocene boundary.

Summary

The history of the Messinian salinity crisis can be understood by the interaction of tectonic closure, glacio-eustatic changes, and local climate within the Mediterranean [*Rouchy and St. Martin*, 1992]. These forcing mechanisms operate on different time scales with tectonic closure of the Iberian and Rifian Seaways occurring on time scales of millions of years, and glacio-eustatic and local climatic changes occurring on time scales of tens to hundreds of thousands of years. Tectonic convergence between Africa and Europe gradually narrowed the Iberian and Rifian Seaways during the late Miocene, setting the stage for the salinity crisis. A climatic trend toward increased aridity and continentality during

the late Miocene (as reflected by the increased importance of C-4 ecosystems and the late Miocene carbon shift) may have also predisposed the Mediterranean to desiccation. The increases in $\delta^{18}O$ values at 7.17 and 6.8 Ma (Figure 12) mark a decrease in bottom water temperature in the Rifian Strait and a change in glacial boundary conditions that lowered sea level and resulted in the establishment of a negative water budget in the Mediterranean. This change is recorded by the faunal and isotopic proxies in northwest Morocco, which document an important current reversal in deep-water flow through the Rifian Corridor near the Tortonian/Messinian boundary [*Hodell et al.*, 1989; *Benson et al.*, 1991]. The increase in $\delta^{18}O$ values at 6.8 Ma correlates to the base of the Tripoli Formation in the Mediterranean, and the onset of crisis conditions [*McKenzie et al.* 1979/1980].

The $\delta^{18}O$ signal during the Messinian is marked by 40-kyr cyclicity that is interpreted as representing ice volume variations at high latitudes that are responding to insolation forcing by orbital obliquity (41-kyr cycle). Associated sea level rises and falls may have influenced the flow of marine waters into the Mediterranean during the Messinian. Local precessional forcing of climate in the Mediterranean at 19 and 23 kyr was undoubtedly superimposed upon any glacio-eustatic changes. The cyclic nature of the oxygen isotope signal permits us to define oxygen isotope stages from stage TG24 in Chron C3r (earliest Gilbert) to stage C3Ar.$\delta^{18}O$.18 at the top of Chron C3Bn (6.935 Ma). This oxygen isotope stratigraphy provides a high-resolution chronology for the Messinian stage and serves as a template against which cycles in the Mediterranean can be compared once they have been enumerated.

The greatest $\delta^{18}O$ values (and presumably the most intense glacial stages) of the entire Messinian stage occurred during Chron C3r (the earliest Gilbert) during isotope stages TG 20 and 22 [*Shackleton et al.*, 1994a]. The regressions associated with these events may have resulted in the complete isolation of the Mediterranean from the world ocean [*Shackleton et al.*, 1994a]. Following stage TG12 in the Salé record there exists a trend toward progressively lower $\delta^{18}O$ values that may represents a series of marine transgressions that eventually reflooded the Mediterranean and ended the salinity crisis. The timing of these events are uncertain because of lack of paleomagnetic and biostratigraphic control at the top of the Salé core, but extrapolation of 41-kyr oxygen isotopic cycles from the top of Chron C3An (5.894 Ma) suggests that the decrease in $\delta^{18}O$ values occurred near the Miocene/Pliocene boundary. We conclude that the general trends in $\delta^{18}O$ and inferred changes in global ice volume are consistent with scenarios calling for at least partial control of the Messinian salinity crisis by fluctuations in global sea level.

Acknowledgments. This work was sponsored by the Smithsonian Institution and the National Geographic Society and by a Presidential Young Investigator award from the National Science Foundation (grant OCE 88-58012) to D.A.H. A Doherty Senior Scientist award and NSF grant OCE94-04447 to D.V.K. provided support for paleomagnetic analyses. We thank the Moroccan Geological Survey for logistical support, Roberto Mazzei for nannofossil identifications, and Gioacchino Bonaduce for overseeing drilling operations. The paper benefited by thoughtful reviews by F. Hilgen and an anonymous referee. LDEO Contribution 5262.

References

Adams, C. G., R. H. Benson, R. B. Kidd, W. B. F. Ryan, and R. C. Wright, The Messinian Salinity Crisis and evidence of late Miocene eustatic changes in the world ocean, *Nature, 269*, 383-386, 1977.

Aharon, P., S. L. Goldstein, C. W. Wheeler, and G. Jacobson, Sea-level events in the South Pacific linked with the Messinian salinity crisis, *Geology, 21*, 771-775, 1993.

Aïssaoui, D. M., and J. L. Kirschvink, Atoll magnetostratigraphy: Calibration of their eustatic records, *Terra Nova, 308*, 614-617, 1991.

Baksi, A. K., A geomagnetic polarity time scale for the period 0-17 Ma, based on $^{40}Ar/^{39}Ar$ plateau ages for selected field reversals, *Geophys. Res. Lett., 20*, 1607-1610, 1993.

Barker, *et al.*, *Proceedings of ODP, Initial Reports*, vol. *113*, Ocean Drilling Program, College Station, Tex., 1988.

Barron, J. A., and G. Keller, Paleotemperature oscillations in the middle and late Miocene of the northeastern Pacific, *Micropaleontology, 29*, 150-181, 1983.

Benson, R. H., Messinian salinity crisis, *Encyclopedia of Earth System Science, 3*, 161-167, 1991.

Benson, R. H., and K. Rakic-El Bied, Biodynamics, saline giants and late Miocene catastrophism, *Carbonates Evaporites, 6*(2), 127-168, 1991a.

Benson, R. H., and K. Rakic-El Bied, The Messinian parastratotype at Cuevas del Almanzora, Vera Basin, SE Spain: Refutation of the deep-basin, shallow-water hypothesis?, *Micropaleontology, 37*, 289-302, 1991b.

Benson, R. H., and D. A. Hodell, Comment on "A critical re-evaluation of the Miocene/Pliocene boundary as defined in the Mediterranean", *Earth Planet. Sci. Lett., 124*, 245-250, 1994.

Benson, R. H., K. Rakic-El Bied, and G. Bonaduce, An important current reversal (influx) in the Rifian Corridor (Morocco) at the Tortonian-Messinian Boundary: The end of the Tethys Ocean, *Paleoceanography, 6*(1), 164-192, 1991.

Berger, W. H., and E. Vincent, Deep-sea carbonates: Reading the carbon-isotope signal, *Geol. Rundsch., 75*, 249-269, 1986.

Berggren, W. A., D. V. Kent, and J. A. van Couvering, Neogene geochronology and chronostratigraphy, in *Geochronology and the Geologic Time Scale*, edited by N. J. Snelling, pp. 211-260, Geological Society of London, London, 1985.

Bizon, G., and J.-J. Bizon, Atlas des Principaux Foraminiferes Planctoniques du Bassin Méditerranéen (Oligocene a Quaternaire), pp. 1-316, Technip, Paris, 1972.

Borsetti, A. M., P. V. Curzi, V. Landuzzi, M. Mutti, F. Ricci Lucchi, R. Sartori, L. Tomadin, and G. G. Zuffa, Messinian and pre-Messinian sediments from ODP Leg 107 sites 652 and 654 in the Tyrrhenian Sea: Sedimentologic and petrographic study and possible comparisions with Italian sequences, *Proc. Ocean Drill. Prog., Sci. Results, 107*, 169-186, 1990.

Bossio, A., R. Mazzanti, R. Mazzei, and G. Savatorini, Analsi micropaleontologiche della formationi mioceniche, plioceniche e pleistoceniche dell'area del Comune de Rosignano M., in *La Scienza dell Terra, Novo Strumentot per la Lettura e Pianificazoione del Territorio del Comene di Rosignano M., Suppl. 1, Quad. Mus. St. Nat. Liverno, 6*, 1985.

Bossio, A., K. El Bied-Rakic, L. Gianelli, R. Mazzei, A. Russo, and G. Salvatorini, Correlation de quelques sections stratigraphiques du bassin Méditerranéen sur la base des Foraminiferes planktoniques, Nannoplancton calcaire et Ostracodes, *Atti. Soc. Tosc. Sc. Nat. Mem., Ser. A., 83*, 121-137, 1976.

Cande, S. C., and D. V. Kent, A new geomagnetic polarity time scale for the Late Cretaceous and Cenozoic, *J. Geophys. Res., 97*, 13917-13951, 1992.

Cerling, T. E., J. Quade, Y. Wang, and J. R. Bowman, Carbon isotopes in soils and palaeosols as paleoecologic indicators, *Nature, 341*, 138-139, 1989.

Channell, J. E. T., D. Rio, R. Sprovieri, and G. Glaçon, Biomagnetostratigraphic correlations from leg 107 in the Tyrrhenian

Sea, *Proc. Ocean Drill. Prog., Sci. Results, 107*, 669-682, 1990a.

Channell, J. E. T., M. Torii, and T. Hawthorn, Magntostratigraphy of sediments recovered at sites 650, 651, 652 and 654 (Leg 107 in the Tyrrhenian Sea), *Proc. Ocean Drill. Prog., Sci. Results, 107*, 335-346, 1990b.

Cita, M.B., The Miocene/Pliocene boundary: History and definition, in *Late Neogene Epoch Boundaries*, edited by T. Saito and L. H. Burckle, pp. 1-30, Micropaleontology Press, New York, 1975.

Cita, M.B., and W. B. F. Ryan, The Bou Regreg Section of the Atlantic coast of Morocco: Evidence, timing and significance of a late Miocene regressive phase, *Riv. Ital. Paleontol., 84* (4), 1051-1082, 1978a.

Cita, M. B., and J. A. McKenzie, The terminal Miocene event, in *Mesozoic and Cenozoic Oceans*, Geodyn. Ser., vol. *15*, edited by K. J. Hsü, pp. 123-140, AGU, Washington, D. C., 1986.

Colalongo, M. L., A. di Grande, S. D'Onofrio, L. Gianelli, S. Iaccarion, R. Mazzei, M. Romeo, and G. Salvatorini, Stratigraphy of Late Miocene Italian sections straddling the Tortonian/Messinian boundary, *Boll. Soc. Paleontol. Ital., 18*, 258-302, 1979.

Cunningham, K. J., M. R. Farr, and K. Rakic-El Bied, Magnetostratigraphic dating of an Upper Miocene shallow-marine and continental sedimentary succession in northeastern Morocco and correlation to regional and global events, *Earth Planet. Sci. Lett.*, in press, 1994.

Engleman, E. E., L. L. Jackson, and D. R. Norton, Determination of carbonate carbon in geological materials by coulometric titration, *Chem. Geol., 53*, 125-128, 1985.

Ehrmann, W. U., M. J. Hambrey, J. G. Baldauf, J. Barron, B. Larsen, A. Mackensen, S. W. Wise Jr., and J. C. Zachos, History of Antarctic glaciation: An Indian Ocean perspective, in *Synthesis of Results from Scientific Drilling in the Indian Ocean, Geophys. Monogr. Ser.*, vol. 70, edited by R. A. Duncan, D. K. Rea, R. B. Kidd, U. von Rad, and J. K. Weissel, pp. 423-446, AGU, Washington, D. C., 1992.

Feinberg, H., and H. G. Lorenz, Nouvelles données stratigraphiques sur le Miocene superieur et le Pliocene du Maroc Nord Occidental, *Notes Serv. Geol. Maroc, 30*(225), 21-26, 1970.

Flores, J. A., Los ceratolitos de algunas secciones del noroeste de la cuenca de Guadalquivir (S.O. de Espana) y sondeos oceanicos (DSDP) adyacentes, *Stud. Geol. Samananticensia, 21*, 167-185, 1985.

Freeman, K. H., and J. M. Hayes, Fractionation of carbon isotopes by phytoplankton and estimates of ancient CO_2 levels, *Global Biogeochem. Cycles, 6*, 185-198, 1992.

Gautier, F., G. Clauzon, J.-P. Suc, J. Cravatte, and D. Violanti, Age et duree de la crise de salinité messinienne, *C. R. Acad. Sci. Paris, 318*, 1103-1109, 1994.

Glacon, G., C. Vergnaud Grazzini, S. Iaccarino, J.-P. Rehault, A. Randrianasolo, J. F. Sierro, P. Weaver, J. Channell, M. Torii, and T. Hawthorne, Planktonic foraminiferal events and stable isotope records in the upper Miocene, Site 654, *Proc. Ocean Drill. Prog., Sci. Results, 107*, 415-428, 1990.

Haq, B. U., J. Hardenbol, and P. R. Vail, Chronology of fluctuating sea level since the Triassic, *Science, 235*, 1136-1167, 1987.

Hays, J. D., T. Saito, N. D. Opdyke, and L. H. Burckle, Pliocene-Pleistocene sediments of the equatorial Pacific: Their palaeomagnetic, biostratigraphic, and climatic record, *Geol. Soc. Am. Bull., 80*, 1481-1514, 1969.

Hilgen, F. J., Extension of the astronomically calibrated (polarity) time scale to the Miocene/Pliocene boundary, *Earth Planet. Sci. Lett., 107*, 349-368, 1991a.

Hilgen, F. J., Astronomical calibration of Gauss to Matuyama sapropels in the Mediterranean and implications for the Geomagnetic Polarity Time Scale, *Earth Planet. Sci. Lett., 104*, 226-244, 1991b.

Hilgen, F. J., Sedimentary rhythms and high-resolution chronostratigraphic correlations in the Mediterranean Pliocene, *Newsl. Stratigr., 17(2)*, 109-127, 1987.

Hilgen, F. J., and C. G. Langereis, A critical re-evaluation of the Miocene/Pliocene boundary as defined in the Mediterranean, *Earth Planet. Sci. Lett., 118*, 167-169, 1993.

Hodell, D. A., and J. P. Kennett, Late Miocene-early Pliocene stratigraphy and paleoceanography of the South Atlantic and southwest Pacific oceans: A synthesis, *Paleoceanography, 1*(3), 285-311, 1986.

Hodell, D. A., R. H. Benson, J. P. Kennett, and K. Rakic-El Bied, Stable isotope stratigraphy of Late Miocene-Early Pliocene sequences in Northwest Morocco: The Bou Regreg Section, *Paleoceanography, 4*(4), 467-482, 1989.

Hodell, D. A., K. M. Elmstrom, and J. P. Kennett, Latest Miocene benthic $\delta^{18}O$ changes, global ice volume, sea level, and the Messinian salinity crisis, *Nature, 320*, 411-414, 1986.

Hooper, P. W. P., and P. P. E. Weaver, Paleoceanographic significance of late Miocene to early Pliocene planktonic foraminifers at Deep Sea Drilling Project Site 609, *Initial Rep. Deep Sea Drill. Proj., 94*, 925-934, 1987.

Hsü, K. J., When the Mediterranean Sea dried up, *Sci. Am., 277*, 27-36, 1972.

Hsü, K. J., W. B. F. Ryan, and M. B. Cita, Late Miocene dessication of the Mediterranean, *Nature, 242*(5395), 240-244, 1973.

Imbrie, J., J. D. Hays, D. G. Martinson, A. McIntyre, A. C. Mix, J. J. Morley, N. G. Pisias, W. L. Prell, and N. J. Shackleton, The orbital theory of Pleistocene climate: Support from a revised chronology of the marine $\delta^{18}O$ record, in *Milankovitch and Climate, NATO ASI Ser.*, vol. 126, edited by A. Berger, J. Imbrie, J. Hays, G. Kukla, and B. Saltzman, pp. 269-305, D. Riedel, Hingham, Mass., 1984..

Ingle, J. C., Foraminiferal biofacies variation and the Miocene-Pliocene boundary in southern California, *Am. Paleontol. Bull., 52*, 217-394, 1967.

Jansen, E., and J. Sjøholm, Reconstruction of glaciation over the past 6 Myr from ice-borne deposits in the Norwegian Sea, *Nature, 349*, 600-603, 1991.

Jenkins, G. M., and D. G. Watts, *Spectral Analysis and Its Applications*, 525 pp., Holden-Day, San Francisco, Calif., 1968.

Kastens, K. A., Did a glacio-eustatic sea level drop trigger the Messinian salinity crisis? New evidence from Ocean Drilling Program site 654 in the Tyrrhenian Sea, *Paleoceanography, 7*, 333-356, 1992.

Kastens, K. A., and J. Mascle, The geological evolution of the Tyrrhenian Sea: An introduction to the scientific results of ODP leg 107, *Proc. Ocean Drill. Prog., Sci. Res., 107*, 3-28, 1990.

Keigwin, L. D., Jr., Toward a high-resolution chronology for latest Miocene paleoceanographic events, *Paleoceanography 2*(6), 639-660, 1987.

Keigwin, L. D., Jr, and N. J. Shackleton, Uppermost Miocene carbon isotope stratigraphy of a piston core in the equatorial Pacific, *Nature, 284*, 613-614, 1980.

Kennett, J. P., Recognition and correlation of the Kapitean Stage (upper Miocene, New Zealand), *N. Z. J. Geol. Geophys., 10*, 1051-1063, 1967.

Kennett, J. P., and P. F. Barker, Latest Cretaceous to Cenozoic climate and oceanographic development in the Weddell Sea, Antarctica: An ocean-drilling perspective, *Proc. Ocean Drill. Prog., Sci. Res., 113*, 937-960, 1990.

Kennett, J. P., and P. Vella, Late Cenozoic planktonic foraminifera and paleoceanography at DSDP site 284 in the cool subtropical South Pacific, *Initial Repts. Deep Sea Drill. Proj., 29*, 769-800, 1975.

Kennett, J. P., and N. D. Watkins, Late Miocene-early Pliocene paleomagnetic stratigraphy, paleoclimatology, and biostratigraphy in New Zealand, *Geol. Soc. Am. Bull., 85*, 1385-1398, 1974.

Kirschvink, J., The least-squares line and plane and the analysis of magnetic data, *Geophys. J. R. Astr. Soc., 62*, 699-718, 1980.

Krijgsman, W., F. J. Hilgen, C. G. Langereis, and W. J. Zachariasse, The age of the Tortonian/Messinian boundary, *Earth Planet. Sci. Lett., 121*, 533-547, 1994.

Langereis, C. G., and M. J. Dekkers, Paleomagnetism and rock magnetism of the Tortonian-Messinian boundary stratotype at

Falconara, Sicily, *Phys. Earth Planet. Inter.*, *71*, 100-111, 1992.

Larsen, H. C., A. D. Saunders, P. D. Clift, J. Beget, W. Wei, S. Spezzaferri, *et al.*, Seven million years of glaciation in Greenland, *Science*, *264*, 952-955, 1994.

Loutit, T. S., and L. D. Keigwin, Jr., Stable isotopic evidence for latest Miocene sea level fall in the Mediterranean region, *Nature*, *300*, 163-166, 1982.

Lutze, G. F., Depth distribution of benthonic foraminifera from the continental margin off Northwest Africa, *Meteor Forschung., Reihe C*, *32*, 31-80, 1980.

Mazzei, R., I. Raffi, N. Hamilton, and M. B. Cita, Calibration of Late Neogene calcarious nannoplankton datum planes with the paleomagnetic record of site 397 and correlation with Moroccan and Mediterranean sections, *Init. Repts. Deep Sea Drilling Proj.*, *47*, 376-389, 1979.

McKenzie, J. A., and H. Oberhansli, Paleoceanographic expression of the Messinian salinity crisis, in *South Atlantic Paleoceanography*, edited by K. J. Hsü and H. J. Weissert, pp. 99-123, Cambridge Univ. Press, Cambridge, 1985.

McKenzie, J. A., and R. Sprovieri, Paleoceanographic conditions following the earliest Pliocene flooding of the Tyrrhenian Sea, *Proceedings Ocean Drill. Prog.ram Sci. Results*, *107*, 405-414, 1990.

McKenzie, J. A., H. C. Jenkyns, and G. G. Bennet, Stable isotope study of the cyclic diatomite-claystones from the Tripoli Formation, Sicily: A prelude to the Messinian Salinity Crisis, *Palaeogeogr. Palaeoclimatol. Palaeoecol.*, *29*, 125-141, 1979/1980.

Moreau, M. G., H. Feinberg, and J. P. Pozzi, Magnetobiostratigraphy of a Late Miocene section from the Moroccan Atlantic margin, *Earth Planet. Sci. Lett.*, *76*, 167-175, 1985.

Müller, D. W., and K. J. Hsü, Event stratigraphy and paleoceanography in the Fortuna basin (southeast Spain): A scenario for the Messinian salinity crisis, *Paleoceanography*, *2*(6), 679-696, 1987.

Müller, D. W., and P. A. Mueller, Origin and age of the Mediterranean Messinian evaporites: Implications for Sr isotopes, *Earth Planet. Sci. Lett.*, *107*, 1-12, 1991.

Müller, D. W., D. A. Hodell, and P. F. Ciesielski, Late Miocene to earliest Pliocene (9.8-4.5 Ma) paleoceanography of the subantarctic Southeast Atlantic: Stable isotopic, sedimentologic, and microfossil evidence, *Proc. Ocean Drill. Prog. Sci. Res.*, *114*, 459-474, 1991.

Pedley, H. M., and M. Grasso, Controls on faunal and sediment cyclicity within the Tripoli and Calcare di Base basin (Late Miocene) of central Sicily, *Palaeogeogr. Palaeoclimatol. Palaeoecol.*, *105*, 337-360, 1993.

Pierre, C., and J. M. Rouchy, Sedimentary and diagenetic evolution of Messinian evaporites in the Tyrrhenian Sea (ODP Leg 107, Sites 652, 653, and 654): Petrographic, mineralogical, and stable isotope records, *Proc. Ocean Drill. Prog., Sci. Res.*, *107*, 187-210, 1990.

Pisias, N. G., and A. C. Mix, Aliasing of the geologic record and the search for long-period Milankovitch cycles, *Paleoceanography*, *3*, 613-619, 1988.

Quade, J., T. E. Cerling, and J. R. Bowman, Development of Asian monsoon revealed by marked ecological shift during the latest Miocene in northern Pakistan, *Nature*, *342*, 163-166, 1989.

Raymo, M. E., W. F. Ruddiman, J. Backman, B. M. Clement, and D. G. Martinson, Late Pliocene variation in northern hemisphere ice sheets and North Atlantic deepwater circulation, *Paleoceanography*, *4*, 413-446, 1989.

Rau, G.H., T. Takahashi, and D.J. Des Marais, Latitudinal variations in plankton $\delta^{13}C$: Implications for CO_2 and productivity in past oceans, *Nature*, *341*, 516-518, 1989.

Retallack, G. J., Late Miocene global isotopic shift and expansion of tall grasslands, *Geol. Soc. Am. Abstract Programs*, *25*(6), A131, 1993.

Rouchy, J. M., and J. P. St. Martin, Late Miocene events in the Mediterranean as recorded by carbonate-evaporite relations, *Geology*, *20*, 629-632, 1992.

Ruddiman, W. F., M. E. Raymo, D. G. Martinson, B. M. Clement, and J. Backman, Pleistocene evolution of Northern Hemisphere climate, *Paleoceanography*, *4*, 353-412, 1989.

Ryan, W. B. F., M. B. Cita, M. D. Rawson, L. H. Burckle, and T. Saito, A paleomagnetic assignment of Neogene stage boundaries and the development of isochronous datum planes between the Mediterranean, the Pacific and Indian Oceans in order to investigate the response of the world ocean to the Mediterranean salinity crisis, *Riv. Ital. Paleontol.*, *80*, 631-687, 1974.

Saito, T., L. H. Burckle, and J. D. Hays, Late Miocene to Pleistocene biostratigraphy of equatorial Pacific sediments, in *Late Neogene Epoch Boundaries*, edited by T. Saito, and L. H. Burckle, pp. 226-244, Micropaleontology Press, New York, 1975.

Schlesinger, W.H., *Biogeochemistry: An Analysis of Global Change*, 443 pp., Academic, San Diego, Calif., 1991.

Scott, G. H., Upper Miocene biostratigraphy: Does *Globorotalia conomiozea* occur in the Messinian?, *Riv. Espag. Micropaleontol.*, *12*, 489-506, 1980.

Shackleton, N. J., and J. P. Kennett, Late Cenozoic oxygen and carbon isotopic changes at DSDP site 284: Implications for glacial history of the northern hemisphere and Antarctica, *Initial Rep. Deep Sea Drill. Proj.*, *29*, 801-807, 1975.

Shackleton, N. J., M. A. Hall, and D. Pate, Pliocene stable isotope stratigraphy of ODP site 846, *Proc. Ocean Drill. Prog. Sci. Res.*, 1994a.

Shackleton, N. J., S. Crowhurst, T. Hagelberg, N. G. Pisias, and D. A. Schneider, A new late Neogene time scale: Application to leg 138 sites, *Proc. Ocean Drill. Prog. Sci. Res.*, 1994b.

Sierro, F. J., The replacement of the *"Globorotalia menardii"* group by the *"Globorotalia miotumida"* group: An aid to recognizing the Tortonian/Messinian boundary in the Mediterranean and adjacent Atlantic, *Mar. Micropaleontol.*, *9*, 525-535, 1985.

Sierro, F. J., J. A. Flores, J. Civis, J. A. González Delgado, and G. Francés, Late Miocene globorotaliid event-stratigraphy and biogeography in the NE-Atlantic and Mediterranean, *Mar. Micropaleontol.*, *21*, 143-168, 1993.

Stainforth, R. M., J. L. Lamb, H. P. Luterbacher, J. Beard, and R. M. Jeffords, Cenozoic planktonic foraminiferal zonations and characteristic index forms, *Univ. Kans. Paleontol. Contrib. Pap.*, *60*, 1-425, 1975.

Suc, J. P., Flores Néogènes de Méditerranée Occidentale, Climat et Paléogéographie, *Bull. Centres Rech. Explor.-Prod.*, Elf-Aquitaine, *10*, 477-488, 1986.

Suc, J. P., Distribution latitudinale et étagement des associations végétales au Cénozoïque supérieur dans l'aire ouest-méditerranéenne, *Bull. Soc. Géol. Fr.*, *1989*, 541-550, 1989.

Suc, J. P., and E. Bessais, Pérennité d'un climat thermo-xéric en Sicile avant, pendant, après la crise de salinité messinienne, *Compte Rendus Acad. Sci. Paris*, *310*, ser. II, 1701-1707, 1990.

Tauxe, L., J. Besse, and J. L. LaBrecque, Paleolatitudes from DSDP Leg 3 cores: Implications for the apparent polar wander path for Africa during the late Mesozoic and Cenozoic, *Geophys. J. R. Astron. Soc.*, *73*, 315-324, 1983.

Thunell, R. C., D. F. Williams, and M. Howell, Atlantic-Mediterranean water exchange during the late Neogene, *Paleoceanography*, *2*(6), 661-678, 1987.

Thunell, R. C., D. Rio, R. Sprovieri, and C. Vergnaud-Grazzini, An overview of the post-Messinian paleoenvironmental history of the western Mediterranean, *Paleoceanography*, *6*, 143-164, 1991.

Vincent, E., J. S. Killingley, and W. H. Berger, The Magnetic Epoch 6 carbon shift: A change in the ocean's $^{13}C/^{12}C$ ratio 6.2 million years ago, *Mar. Micropaleontol.*, *5*, 185-203, 1980.

Wolfe, J. A., and D. M. Hopkins, Climatic changes recorded by Tertiary land floras in Northwestern North America, in *Tertiary Correlations and Climatic Changes in the Pacific*, edited by K. Hatai, pp. 67-76, Sasaki, Tokyo, Japan, 1967.

Zachariasse, W. J., Planktonic foraminiferal biostratigraphy of the Neogene of Crete (Greece), *Utrecht Micropaleontol. Bull.*, *11*, 1-171, 1975.

Zahn, R., M. Sarnthein, and H. Erlenkeuser, Benthic isotope evidence for changes of the Mediterranean outflow during the late Quaternary, *Paleoceanography*, 2(6), 543-559, 1987.

R. H. Benson, Smithsonian Institution, U.S. National Museum, MRC:NHB121, Washington, DC 20560. (e-mail:mnhpb039@sivm.si.edu)

A. Boersma, Microclimates, Research Consultants, 540 Gatehill Rd., Stony Point, NY 10980

D. A. Hodell, Department of Geology, 1112 Turlington Hall, University of Florida, Gainesville, FL 32611. (e-mail: hodell@nervm.nerdc.ufl.edu)

D. V. Kent, Lamont-Doherty Earth Observatory, Columbia University, Palisades, NY 10964. (e-mail: dvk@ldgo.columbia.edu)

K. Rakic-El Bied, Smithsonian Institution,, 12 Avenue de France, Rabat, Morocco.

(Received February 15, 1994; revised July 13, 1994; accepted July 13, 1994.)